

PALYNOSTRATIGRAPHY AND PALYNOFACIES OF THE UPPER SILESIAN KEUPER (SOUTHERN POLAND)

Anna FIJALKOWSKA-MADER¹, Carmen HEUNISCH² & Joachim SZULC³

¹ Polish Geological Institute – National Research Institute, Holy Cross Branch, Zgoda 21, 25-953 Kielce, Poland;

e-mail: anna.mader@pgi.gov.pl

² Landesamt für Bergbau, Energie und Geologie, Stillweg 2, 30 655 Hannover, Germany;

e-mail: Carmen.Heunisch@lbeg.niedersachsen.de

³ Institute of Geological Sciences of the Jagiellonian University, Oleandry 2a, 30-063 Kraków, Poland;

e-mail: joachim.szulc@uj.edu.pl

Fijałkowska-Mader, A., Heunisch, C. & Szulc, J., 2015. Palynostratigraphy and palynofacies of the Upper Silesian Keuper (southern Poland). *Annales Societatis Geologorum Poloniae*, 85: 637–661.



Abstract: The results of the palynostratigraphical studies presented in this paper come from five boreholes Patoka 1, Czarny Las, Woźniki Śląskie K1, Kobyłarz 1 and Poreba as well as from four outcrops at Lipie Śląskie, Patoka, Zawiercie and Poreba, in Upper Silesia (southern Poland). The palynostratigraphical zonation presented by Orłowska-Zwolińska (1983) for the epicontinental Upper Triassic of Poland was applied. The palynomorph spectra are marked by different preservation states, combined with the frequent occurrence of reworked specimens, probably even from Palaeozoic strata. The spore-pollen assemblage recognized in the “Chrzanów Formation” belongs to the early Carnian verrucata Subzone of the palynological longdonensis Zone. The spectrum from the Stuttgart Formation represents the Carnian astigmosus Zone. Spectra in the Patoka Marly Mudstone-Sandstone Member (Grabowa Mudstone-Carbonate Formation), with the Lisowice bone-bearing horizon, represent the middle and late Norian meyeriana b Subzone. The Rhaetian age of the bone-bearing succession in the Lisowice–Lipie Śląskie clay-pit suggested in the literature was not confirmed. The age of assemblages from the “Połomia Formation”, which overlies the Patoka Member, was not determined, owing to the poor state of miospore preservation. Moreover, three types of palynofacies were recognized as being characteristic for a fluvial channel (1), a flood plain (2), and lacustrine and playa environments (3) as well as for an undetermined milieu. Type 1 was found in the deposits of the Stuttgart Formation, the Patoka Member and the “Połomia Formation”, type 2 in the Patoka Member and the “Połomia Formation”, type 3 in the “Chrzanów Formation”, the Stuttgart Formation and the Patoka Member.

Key words: Miospores, palynostratigraphy, palynofacies, Upper Triassic, Upper Silesia.

Manuscript received 27 January 2015, accepted 11 July 2015

INTRODUCTION

Palynostratigraphical studies, based on miospores from the Upper Triassic of Upper Silesia (Fig. 1), were initiated by Orłowska-Zwolińska (in Grodzicka-Szymanko and Orłowska-Zwolińska, 1972). She recognized three spore-pollen assemblages, here assigned to lithostratigraphic units that are defined below (Fig. 2): Porcellispora longdonensis in the “Chrzanów Formation”, Aulisporites astigmosus in the Stuttgart Formation, and Corollina (= Classopollis; see below) meyeriana in the lower part of the later Grabowa Formation in the Woźniki – Cynków area (E part of the Upper Silesia basin). She further studied several borehole records in the Zawiercie and Chrzanów areas (Orłowska-Zwolińska, 1981, 1983). The results of this investigation confirmed the previous palynostratigraphy.

The next studies were carried out by Heunisch, who recognized the meyeriana b Subzone in six out of the eight samples analyzed (these results are presented in part in Szulc *et al.*, 2006). The same age was suggested by Staneczko (2007) for the miospore spectrum from the Lipie Śląskie clay-pit near Lubliniec, also known in the literature as the Lisowice clay-pit. Dzik *et al.* (2008a, b) noted the presence of the two miospore species *Brachysaccus neomundanus* (Leschik) Mäder and *Monosulcites minimus* Cookson in the Lipie Śląskie and, on the basis of their doubtful connection to the macroflora, assumed a Rhaetian age for them (see Szulc *et al.* 2015). Świło *et al.* (2014) presented a list of miospores also from Lipie Śląskie clay-pit, representing the uppermost meyeriana Zone (= meyeriana c Subzone). Wawrzyniak (in

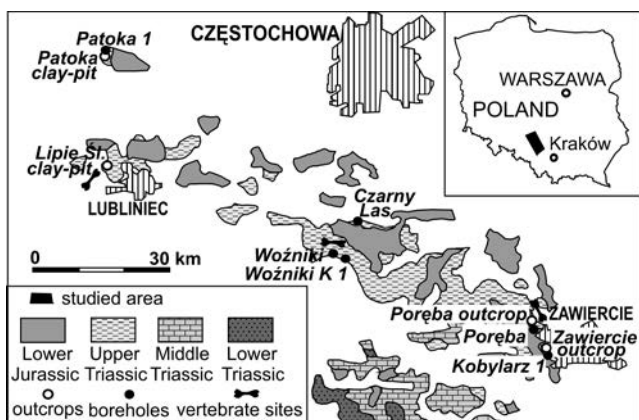


Fig. 1. Location of boreholes and outcrops studied on a geological map, showing surface distribution of Triassic to Lower Jurassic strata (after fig. 1 in Szulc and Racki, 2015).

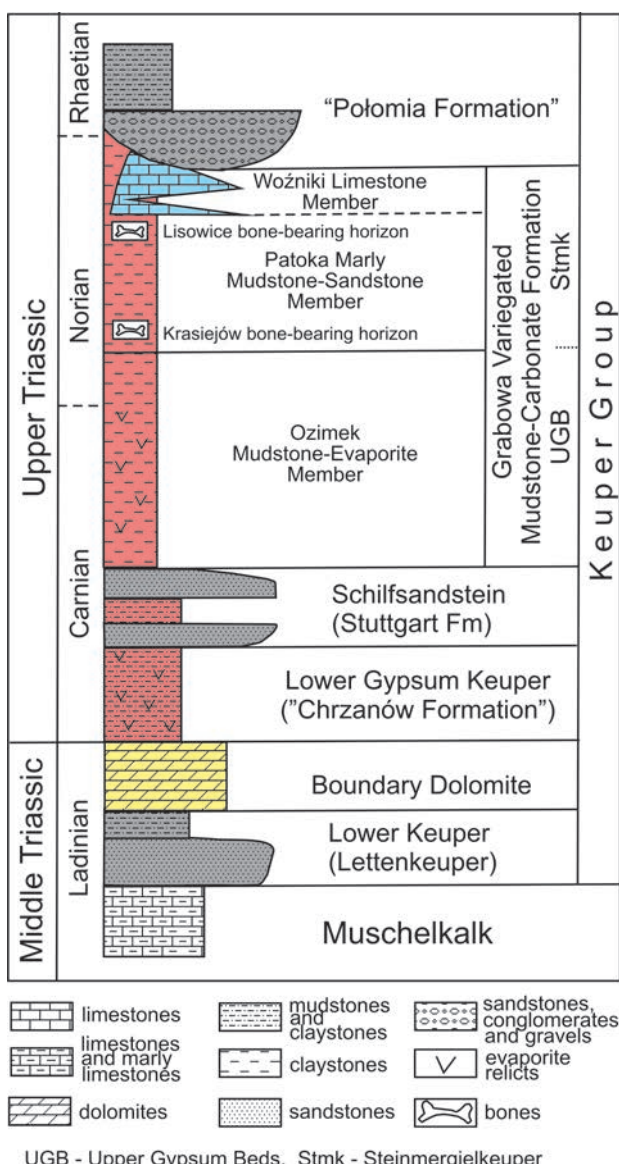


Fig. 2. Schematic lithostratigraphic section of the Upper Triassic of Upper Silesia; thicknesses are not to scale; modified from Szulc and Racki (2015, fig. 2); partly after Becker *et al.* (2008).

Sadlok and Wawrzyniak, 2013) reported an assemblage of the probable meyeriana b Subzone at the Zawiercie-Marciszów outcrop. In the most recent paper on the subject, Pieńkowski *et al.* (2014) assumed that the deposits at the Lipie Śląskie location represent the meyeriana c Subzone as well as the succeeding Riccisporites tuberculatus Zone.

Palynostratigraphical investigations of the Upper Triassic were continued by Fijałkowska-Mader, in connection with a multidisciplinary grant to G. Racki with a focus on integrative Upper Silesian Keuper stratigraphy, and the results, complemented with unpublished material by Heunisch, are presented in this paper. The samples are from the complete composite middle-upper Keuper succession, derived mostly from the lithologic records of four boreholes: Patoka 1, Woźniki K1, Kobylarz 1 and Poręba (Fig. 1), with an emphasis on the bone-bearing, variegated deposits of Grabowa Mudstone-Carbonate Formation (Fig. 2), a unit of Bilan (1976), recently redefined by Szulc and Racki (2015).

LITHOFACIES SUCCESSION AND GENERAL SETTING OF THE SEDIMENTARY ENVIRONMENTS

The Upper Triassic succession of the study area was formed in the marginal part of the Mid-Polish Basin. Therefore, its thickness is distinctly less than that at the basin centre and erosional and sedimentary gaps are more common. It is also worthy of note that the bone-bearing, alluvial facies are more frequent here than in the central part of the basin.

The lithofacies succession of the Upper Triassic in Upper Silesia is typical for the Germanic domain and reflects the main climatic fluctuations that took place across the Western Tethys domain during Carnian–Rhaetian times (Feist-Burkhardt *et al.*, 2008). The arid phase, in early Carnian times, is recorded as evaporitic sediments of the “Chrzanów Fm” of Bilan (1976), which is correlated with the Lower Gipskeuper in other parts of Poland and the Grabfeld Formation in NW Germany (Becker *et al.*, 2008). The unit is composed of variegated mudstones and claystones containing evaporites, mostly sulphates with subordinate amounts of dolomite (Fig. 2).

The mid-Carnian was characterized by the re-establishment of a humid climate, as indicated by sedimentological and palaeontological data. Pluvialisation resulted in fluvial activity, forming the braided/anastomosing river network of the Stuttgart Fm (the Schilfsandstein) in the Germanic Basin. Sedimentation, typical of dry climatic conditions, characterized the late Carnian and early Norian, evaporite-bearing red beds of the Ozimek Member (= the Upper Gipskeuper) and was dominant in the Germanic Basin.

During mid- and late Norian times, the climate in the Germanic Basin underwent gradual amelioration, as indicated by punctuated sedimentation of evaporite-bearing red-bed facies and their replacement by fluvial sediments, typical for the Steinmergelkeuper facies complex (= the Patoka Member, an equivalent of the Arnstadt Formation; Szulc and Racki, 2015; see also Bilan, 1976; Szulc *et al.*, 2006). The fluvial intervals are particularly well developed at the basin margin, where they formed the alluvial complex of the Löwenstein Formation.

The gradual climatic change could be ascribed to the drift of Middle Europe into a higher palaeolatitudinal position. The Polish basin definitely migrated outside the subtropical dry belt in the latest Norian–Rhaetian times, as indicated by the complete decline of evaporitic sedimentation and by the dominance of siltstones with coal seams and abundant plant debris, typical for the uppermost part of Grabowa Fm and the fluvial quartz sandstones and gravels of the “Połomia Formation” (= Exter Formation), as noted by Grodzicka-Szymanko and Orłowska-Zwolińska (1972) Bilan (1976), Deczkowski (1997) and Szulc and Racki (2015).

MATERIAL AND METHODS

Fifty-nine samples were examined from cores of the Kobylarz 1 (11 samples from a depth of 1.5–30.0 m), Woźniki K1 boreholes (16 samples; 68.8–99.5 m; Fig. 3) and Patoka 1 (32 samples; 17.4–208.0 m; Fig. 4), but only twenty-eight yielded palynological material. This material was complemented with eight productive samples, out of the 41 elaborated by Carmen Heunisch (in Szulc *et al.*, 2006), from the three boreholes: Woźniki (1 sample from a depth of 30.0 m), Poręba (3 samples; 7.7–11.4 m) and Czarny Las (1 sample; 9.7 m) as well as the two outcrops, at the Lipie Śląskie clay-pit, also known in literature as Lisowice (2 samples), and at Zawiercie (1 sample). Four additional samples were taken from the Lipie Śląskie clay-pit, one sample from the Poręba outcrop and two samples from the clay-pit at Patoka (Figs 1, 5).

The rock material was treated according to the method described by Orłowska-Zwolińska (1983). In general, 200 sporomorphs were counted in each sample for quantitative analysis. Only in very sparse spectra, all sporomorphs were counted. For palynofacies analysis, 200 palynomorphs and organic particles were counted per slide.

THE UPPER TRIASSIC PALYNOLOGICAL ZONES DISTINGUISHED IN THE POLISH BASIN AND CORRELATION OF THEM

The palynostratigraphic scheme of Orłowska-Zwolińska (1983, 1985), which is the most suitable for the Polish epicontinental Triassic, was applied. Four palynological zones were distinguished in this scheme in the Upper Triassic: longdonensis (l) in the Boundary Dolomite and Lower Gipskeuper, astigmosus (a) in the Schilfsandstein; meyeriana (m) in the Upper Gipskeuper, Jarkowo and Zbąszynek Beds; and tuberculatus (t) in the Wielichowo Beds. The longdonensis Zone contains two subzones, iliacoidea (li) and verrucata (lv), whereas the meyeriana Zone is divided into three subzones (Fig. 6), a (ma), b (mb) and c (mc).

The base of the longdonensis Zone as well as the iliacoidea Subzone is defined by the first appearances (FADs) of *Porcellispora longdonensis*, *Echinitosporites iliacoidea*, *Duplicisporites granulatus* and *Praecirculina granifer* (see the list of the miospore species in Appendix 1) and the first common occurrence of *Ovalipollis*. The lowermost part of the iliacoidea Subzone, containing acritarchs, is found in the

Boundary Dolomite, whereas its upper part, with the FAD of *Camerosporites secatus*, is in the lower part of Lower Gipskeuper. The last occurrences (LODs) of *E. iliacoidea* and *Eucommiidites microgranulatus* determinate the top of the iliacoidea Subzone.

The verrucata Subzone corresponds with the acmes of the *Triadispora verrucata* and *Ovalipollis ovalis*. The top of the longdonensis Zone and verrucata Subzone is defined by the LODs of *Duplicisporites granulatus*, *Partitisporites maljavkinae*, *Triadispora plicata* and *T. verrucata* (Orłowska-Zwolińska, 1983, 1985). The verrucata Subzone is found in the upper part of the Lower Gipskeuper.

The lowermost part of the iliacoidea Subzone is correlated with the top of the *Heliosaccus dimorphus* Zone *sensu* Herngreen (2005) and the top of the “Geological Time Scale” (GTS) *Heliosaccus dimorphus* Zone (Ogg, 2012) and its upper part and the verrucata Subzone with the *Triadispora verrucata* Subzone of the *Camerosporites secatus* Zone *sensu* Herngreen (2005; see e.g., Kürschner and Herngreen, 2010) as well as with the lower part of the GTS *Camerosporites secatus* Zone (Ogg, 2012; Fig. 6).

The astigmosus Zone corresponds with the acme of *Aulisporites astigmosus* and includes the FADs of *Annulisporites microannulata*, *Apiculatisporis parvispinosus*, *Camarozonosporites laevigatus*, *C. rufus* and *Stereisporites cicatricosus* as well as the LODs of *Aulisporites astigmosus*, *Accinctisporites ligatus*, the majority of the *Aratrisporites* species (*coryliseminis*, *flexibilis*, *fimbriatus*, *granulatus*, *paraspinosus*, *scabratus*, *saturni*), *Illinitisporites chitonoides*, *Verrucosisporites morulae* and *V. pseudomorulae*. The occurrence of the following is limited to this Zone: *Apiculatisporis firmus*, *Gibbosporites hirsutus*, *G. lativerrucosus*, *Kraeuselisporites* species: *cooksonaelain*, *dentatus*, *litius* and *ramosus*, *Reticulatisporites distinctus*, *Zebrasporites corneolus* and *Z. fimbriatus* (Orłowska-Zwolińska, 1983, 1985). The astigmosus Zone is correlated with the *Auslisporites astigmosus* Subzone of the *Camerosporites secatus* Zone *sensu* Herngreen (2005) and the middle part of the GTS *Camerosporites secatus* Zone (Ogg, 2012; Fig. 6).

Orłowska-Zwolińska (1983, p. 49–50) defined the meyeriana Zone as the acme zone – “...numerous and sometimes mass occurrence of *Corollina meyeriana*...” – in the upper part of the Upper Gipskeuper and the overlying strata. However, the base of the meyeriana Zone and the meyeriana a Subzone may be determined (see Orłowska-Zwolińska, 1983, p. 64) by the FAD of *Classopollis meyeriana* (previously *Corollina meyeriana*; see the discussion in Traverse, 2004), which correlates with the FAD of *Corollina* spp./*Classopollis* spp. This last FAD, according to Heunisch (1999, tab. 1 therein), is located in the upper part of her GTr 15 Zone in the Weser/Arnstadt Formations. Kürschner and Herngreen (2010; fig. 3) placed the FAD of *Classopollis* spp. in the late Tuvalian (Hassberge Formation). Heunisch and Nitsch (2011) found the miospore assemblage of the meyeriana Zone in the Mainhardt Formation and opted for a Tuvalian age for the meyeriana Zone. Cirilli (2010, figs 2, 3 therein), however, located the FAD of the *Classopollis meyeriana* and the base of the *Classopollis meyeriana* Subzone in the earliest Norian. The meyeriana a Subzone is correlated with the top of the *Camerosporites*

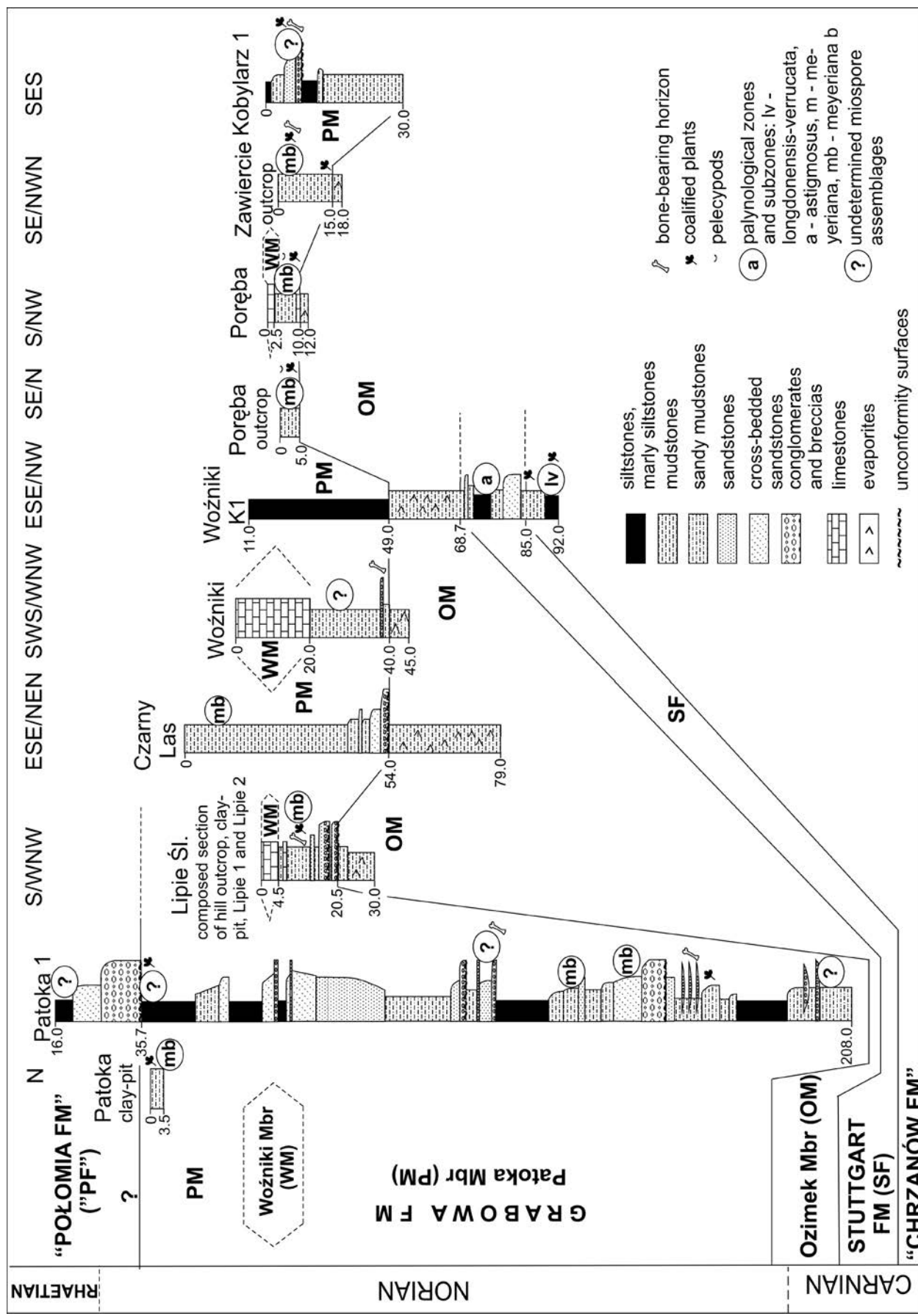


Fig. 5. Lithostratigraphic correlation of the profiles containing miopore assemblages.

CHRONO- STRATI- GRAPHY		LITHOSTRATIGRAPHY W part of the Polish Basin (Becker et al., 2008)	PALYNOSTRATIGRAPHY		
			POLAND (Orłowska-Zwolińska, 1985)	CENTRAL AND NW EUROPE (Kürschner and Herngreen, 2010)	GTS STANDARD ZONES (Ogg, 2012)
TRIASSIC	KEUPER	Wielichowo Beds	tuberculatus	germanicus lundbladii	germanicus
			c	germanicus	
		Zbąszynek Beds	b	rudis	rudis
		Jarkowo Beds	a	secatus	secatus
		Upper Gipskeuper	meyeriana	astigmosus	astigmosus
			long.	verrucata	
		Stuttgart Fm	astigmosus	verrucata	
		Lower Gipskeuper	verrucata	iliacoides	dimorphus
			iliacoides	dimorphus	
		Sulechów Beds	dimorphus	Tasmanites	dimorphus
		UPPER MUSCHELKALK			

L. – LOWER, long. – longdonensis

Fig. 6. Comparison of the Triassic palynological zonation applied in Poland and proposed for Central and Northwestern Europe

secatus Zone *sensu* Herngreen (2005) and the top of the GTS C. secatus Zone (Ogg, 2012; see Fig. 6).

The base of the meyeriana b Subzone is placed at the FADs of *Riccisporites tuberculatus*, *Carnisporites granulatus*, *Heliosporites altmarkensis*, *Monosulcites minimus* and *Neochomotriletes triangularis*. This subzone corresponds with the acmes of *Brachysaccus neomundanus*, *Labiisporites triassicus* and *Nevesisporites limatulus*. Its top is placed at the LODs of *Anapiculatisporites telephorus*, *N. limatulus* and *P. longdonensis*. The subzone is found in the upper part of the Jarkowo Beds and the lower part of the Zbąszynek Beds (Orłowska-Zwolińska, 1983, 1985). It is correlated with the top of the Granuloperculatipollis rudis Zone *sensu* Herngreen (2005) and the GTS G. rudis Zone (Ogg, 2012; see Fig. 6).

The meyeriana c Subzone corresponds with the acmes of *C. torosus* and the last common occurrence of *C. meyeriana* as well as *Ovalipollis* and *Enzonatasporites*. Its base is placed at the FAD of *Rhaetipollis germanicus* and the top is defined by the LODs of many taxa common in the Upper Triassic spectra: *Brachysaccus neomundanus*, *Carnisporites mesozoicus*, *Enzonatasporites* species: *manifestus*, *marginalis* and *vigens*, *Labiisporites triassicus*, *Leschikisporites aduncus* and *Taurocuspites verrucatus*. The meyeriana c Subzone occurs in the upper part of the Zbąszynek Beds (Orłowska-Zwolińska, 1983, 1985) and is correlated with the lower part of the Rhaetipollis germanicus Zone *sensu* Kürschner and Herngreen (2010) as well as with the lower part of the GTS R. germanicus Zone (Ogg, 2012; see Fig. 6).

The base of the tuberculatus Zone is defined by the FADs of many species, the ranges of which are limited to this Zone, such as *Cingulizonates rhaeticus*, *Cornutisporites seebergensis*, *Densosporites cavernatus*, *D. fissus*, *Lo-*

photriletes verrucosus, *Limbosporites lundbladii*, *Perinosporites thuringiacus*, *Semiretisporites goethae*, *S. ornatus*, *S. wielichoviensis*, *Triancoraesporites ancorae*, *T. reticulatus*, or continue to the Lower Jurassic *Acanthotriletes varius*, *Chasmatosporites apertus*, *C. rimatus*, *Concavisporites junctum*, *C. juriensis*, *Dictyophyllidites mortoni*, *Lycopodiacyclites rugulatus*, *Lycopodiumsporites reticulumsporites*, *L. semimuris*, *Marattisporites scabrinus*, *Monosulcites punctatus*, *Pisnuspollenites minimus*, *Quadraeculina anellaformi*, and *Zebrasporites interscriptus*. The Zone corresponds to the acme of *Riccisporites tuberculatus*. The *Deltoidospora* specimens as well as *Concavisporites polygonalis* and *Monosulcites minimus* are common. The top of the Zone is placed not only at the LODs of species mentioned above, but also at the LODs of *Anapiculatisporites spiniger*, *Camarozonosporites laevigatus*, *G. rudis*, *C. zwolinskai* and *Lunatisporites rheaticus*. The Zone occurs in the Wielichowo Beds (Orłowska-Zwolińska, 1983, 1985) and is correlated with the Limbosporites lundbladii Subzone of the Rhaetipollis germanicus Zone *sensu* Kürschner and Herngreen (2010) as well as with the upper part of the GTS R. germanicus Zone (Ogg, 2012; see Fig. 6).

DESCRIPTION OF THE MIOSPORE ASSEMBLAGES

On the basis of more than a hundred miospore taxa, recognized in the material analyzed (a complete list is in Appendix 1 and descriptions of new taxa are given in Appendix 2), seventeen miospore assemblages representing three miospore zones were distinguished (Fig. 5).

Miospore assemblage of the longdonensis Zone (lv)

Characteristics: The two index specimens – the moss spore *Porcellispora longdonensis* (e.g., Mader, 1977; Fig. 7A, B) and the pollen *Triadispora verrucata* (Fig. 7T, U) – occur in an assemblage, dominated by the conifer pollen *Ovalipollis*, *Triadispora* (Fig. 7P–S) and *Brachysaccus* (Fig. 7M). Monosaccate pollen, very similar to the Jurassic araucariacean genus *Callialasporites* (Fig. 7H, I), and conifer striatite pollen (Fig. 7K, L), occurred sporadically. Lycopsid *Aratrisporites* specimens (Fig. 7E–G) predominated among the spores.

Occurrence: Woźniki K1, depth 88.5–89.5 m, “Chrzanów Fm” (Figs 3, 5).

Miospore assemblage of the astigmosus Zone (a)

Characteristics: The assemblage is dominated by the index pollen *Aulisporites astigmosus* (Fig. 8F, G). The pollen *Ovalipollis* (Fig. 9O–R) and *Brachysaccus* occurred less frequently. The lycopsid spores *Aratrisporites* (Fig. 9E–H) and *Kraeuselisporites* (Fig. 9B–D) were characteristic and abundant elements of this spectrum. Fern spores assigned to *Todisporites* (Fig. 8E) and the conifer pollen *Triadispora* (Fig. 10D–F) were relatively numerous. The assemblage is strongly diverse, both taxonomically and botanically. It contained, besides the specimens mentioned above, single spores of the ferns *Deltoidospora* (Fig. 8A–C), *Conosmundasporites* (Fig. 8K), *Conbaculatisporites* (Fig. 8N), *Carnisporites* (Fig. 8H), *Leschikisporis*, *Verrucosporites* (Fig. 8I, J); the horsetail *Calamospora* (Fig. 8D), the lycopsids *Anapiculatisporites* (Fig. 8L), *Lycopodiacytidites* (Fig. 8R), and *Lycopodiumsporites* (Fig. 8P) as well as spores of unknown botanical affinity *Corrugatisporites* (Fig. 8O), aff. *Taurocuspites* (Fig. 9A) and aff. *Semiretisporis* (Fig. 8T).

They were accompanied by rare bisaccate pollen, mainly of coniferous affinity, *Illinites* (Fig. 9N), *Parillinites* (Fig. 9U), *Platysaccus* (Fig. 10A, B), *Labiisporites* (Fig. 10G), *Striatobietites* (Fig. 9T) as well as the monosaccate pollen *Enzonalsporites* (Fig. 9J, K) and aff. *Callialasporites* (Fig. 9M). The fresh-water alga *Schizosporis* from the family Zygemataceae occurred commonly (Fig. 10H). Specimens of reworked spores of the early Triassic genus *Densoisporites* (Fig. 10T), acritarchs and ?chitinozoa occurred sporadically (Fig. 10U).

Occurrence: Woźniki K1, depth 77.1–84.45 m, Stuttgart Fm (Figs 3, 5).

Miospore assemblages of the meyeriana b Subzone (mb)

Characteristics: Although there are some strong variations in composition within these assemblages (Figs 11–13), their common feature is the predominance of conifer pollen. Among them, the index species *Classopollis meyeriana* (Fig. 13K, L), *Brachysaccus neomundanus* (Fig. 13C), *Ovalipollis* sp. div. (Fig. 13B) and *Enzonalsporites* sp. div. (Fig. 13A) were the most abundant. The characteristic form is *Granuloperculatipollis rufus* (Fig. 13M, N). Less frequently the pollen *Labiisporites* (Fig. 13G) occurred, accompanied by single pollen specimens of *Alisporites*, *Parillinites* (Fig. 13D), *Platysaccus* (Fig. 13E), *Falcisporites*

(Fig. 13F), aff. *Pinuspollenites*, *Protodiploxyypinus* (alias *Minutosaccus*) (Fig. 13H) and *Cedripites*. Other less frequently encountered pollen included *Classopollis simplex*, *C. torosa*, *Geopolis zwolinskae*, and *Duplicisporites granulatus* (Fig. 13J). Moreover, single specimens of the cycad pollen *Monosulcites* (Fig. 13O, P) and *Cycadopites* were found. Fern spores *Todisporites* (Fig. 11R) predominated among the spores. Other spores, such as aff. *Conosmundasporites* (Fig. 11S), *Cyclotrites* (Fig. 11T) and *Verrucosporites* (Fig. 12A) as well as the lycopsid spores *Densoisporites* (Fig. 12L–P) and *Nevesisporites* (Fig. 12I), occurred less frequently. They were accompanied by single occurrences of *Taurocuspites* (Fig. 12S, T), *Reticulatisporites* (Fig. 12H), *Deltoidospora* (Fig. 12E), *Calamospora*, *Carnisporites*, *Anapiculatisporites* (Fig. 12C, D), *Uvaespores*, *Foveolatiriletes* (Fig. 12G), *Corrugatisporites* (Fig. 12F), *Baculatisporites* (Fig. 11U), *Porcellispora* (Fig. 12B) and *Polyicingulatisporites* (Fig. 12K, R). Specimens of *Microreticulatisporites* sp., *Neoraistrickia* sp., *Pseudoenzonalsporites summus* and *Vallasporites ignacii* seldom occurred. Single reworked acritarchs were found (Fig. 13U). The presence of fungal spores is the distinctive feature of this assemblage. The algae of the genus *Schizosporis* were relatively numerous. Single specimens of the planktonic alga *Botryococcus* were found in the Poręba borehole at a depth of 153.1 m. Charophyta specimens were recognized in a sample from the Patoka clay-pit.

Occurrence: Patoka clay-pit, uppermost part of the Patoka Mbr; Patoka 1 borehole, depth 134.6–153.1 m, Patoka Mbr (Fig. 4); Lipie Śląskie clay-pit, Patoka Mbr below the oncrolite layer (see Szulc et al., 2006; fig. 5); Czarny Las bore-hole, depth 9.7 m, Patoka Mbr; Zawiercie outcrop, Patoka Mbr (see Szulc et al., 2006; Fig. 5); Poręba outcrop and Poręba borehole, depth 7.7–11.4 m, Patoka Mbr (Fig. 5).

Miospore assemblages of undefined palynostratigraphical position

The miospore assemblage found in the Patoka 1 bore-hole, at a depth of 199.00 m in the middle part of the Patoka Mbr (Figs 4, 5), did not contain any index species. It was dominated by the pollen *Ovalipollis* (Fig. 11E–G) and *Brachysaccus*. The pollen *Triadispora* (Fig. 11K, L), *Platysaccus* (Fig. 11I), *Alisporites* (Fig. 11H) and *Enzonalsporites* (Fig. 11D) are less abundant. They were accompanied by single spores of *Calamospora*, *Anapiculatisporites* (Fig. 11B) and *Kraeuselisporites* (Fig. 11C) as well as the alga *Schizosporis* sp. (Fig. 11M). Reworked early Triassic spores (Fig. 11O) and strongly worn out specimens (Fig. 11N, P) occurred in abundance.

The miospore assemblage recognized in the Woźniki borehole, at a depth of 30.00 m, in the Patoka Mbr, contained single, poorly preserved specimens of *Enzonalsporites* sp., *Cycadopites* sp. and *Chasmatosporites* sp., as well as one specimen of the *Riccisporites tuberculatus*, accompanied by the planktonic alga *Botryococcus* sp., dinoflagellate cysts of *Dapcodinium cf. priscum* and fungal spores.

The miospore assemblage found in the Kobylarz 1 bore-hole, at a depth of 7.0–8.5 m, in the Lisowice bone-bearing horizon, was dominated by conifer pollen of the genera *Ova-*

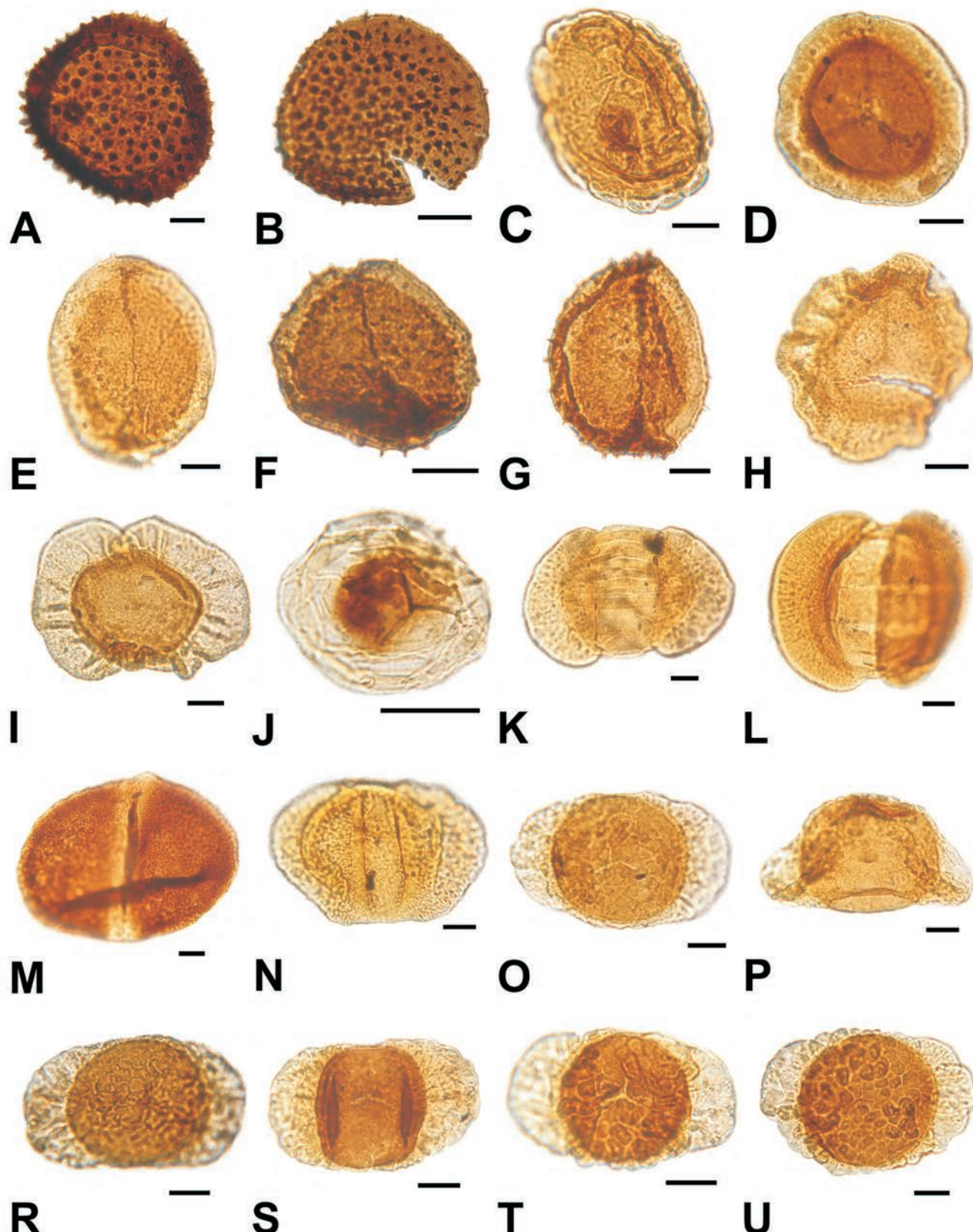


Fig. 7. Miospores from the “Chrzanów Formation” (Carnian), the Woźniki K1 borehole. Scale bar = 10 µm. A, E, G–M, O–T – depth 88.5 m; B–D, F, N, U – depth – 89.5 m. **A, B.** *Porcellispora longdonensis* (Clarke) Scheuring. **C.** aff. *Camerosporites* sp. **D.** *Densosporites* sp. **E.** *Aratrisporites granulatus* (Klaus) Playford et Dettmann. **F, G.** *Aratrisporites paraspinosus* Klaus Dettmann. **H, I.** aff. *Callialasporites*. **J.** aff. *Perinopollenites* sp. **K.** *Striatoabietites balmei* Klaus. **L.** *Infernopalites sulcatus* (Pautsch) Scheuring. **M.** *Brachysaccus neomundanus* (Leschik) Mädlar. **N.** *Parillintes vanus* Scheuring. **O.** *Triadispora crassa* Klaus. **P.** *Triadispora suspecta* Scheuring. **R.** *Triadispora plicata* Klaus. **S.** *Triadispora polonica* Brugman. **T.** *Triadispora verrucata* (Schulz) Scheuring. **U.** *Triadispora verrucata* (Schulz) Scheuring.

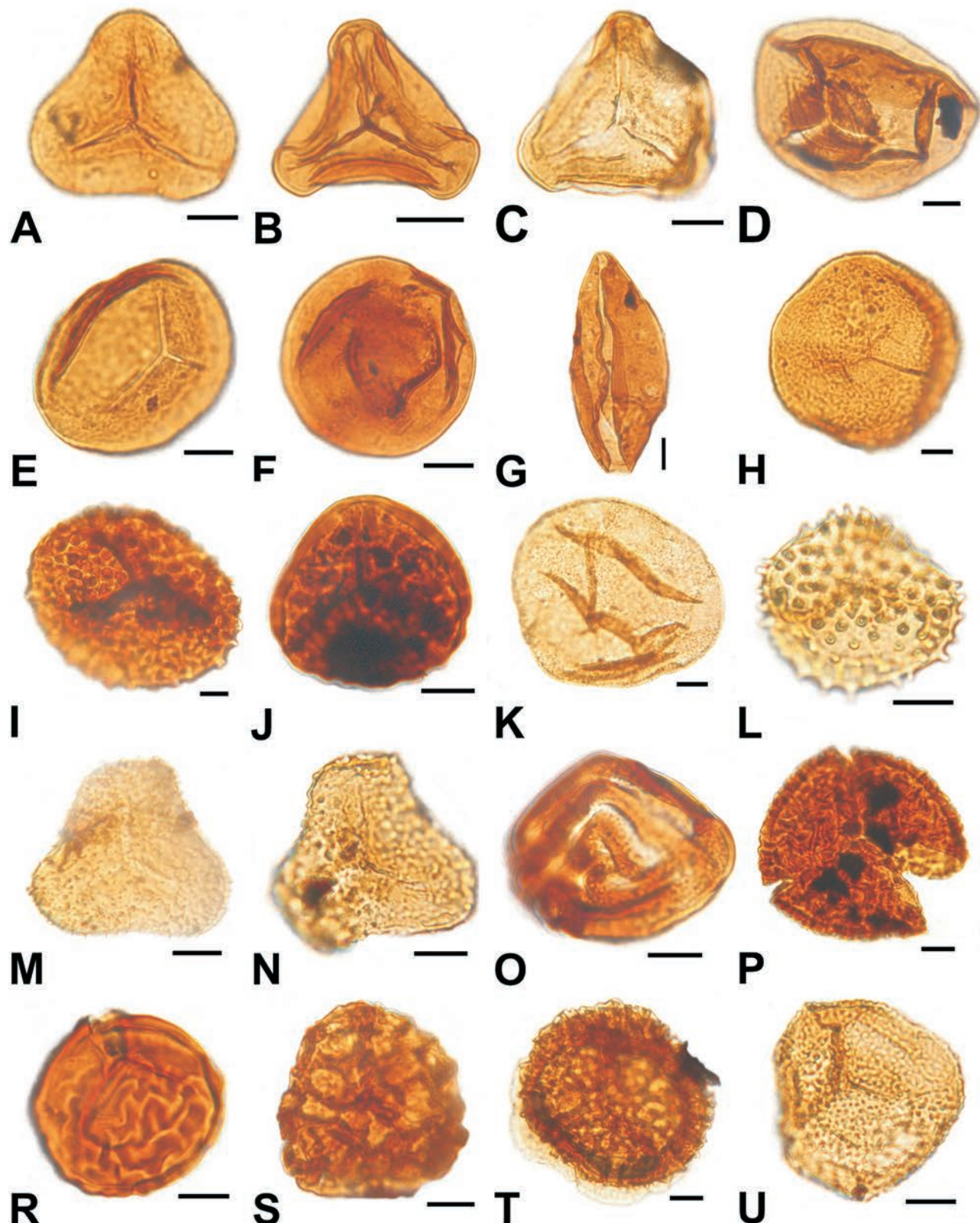


Fig. 8. Miospores from the Stuttgart Formation (Carnian), the Woźniki K1 borehole. Scale bar = 10 µm. B, D, K – depth 77.1 m; F, H, J, L, M, O, S depth – 84.0 m; A, C, E, G, I, N, P, R, T, U – depth 84.45 m. **A.** *Deltoidospora minor* (Couper) Pocock. **B.** *Deltoidospora toralis* (Leschik) Lund. **C.** *Deltoidospora* sp. **D.** *Calamospora tener* (Leschik) de Jersey. **E.** *Todisporites cinctus* (Maliavkina) Orłowska-Zwolińska. **F.** *Aulisporites astigmosus* (Leschik) Klaus. **G.** *Aulisporites astigmosus* (Leschik) Klaus. **H.** *Carnisporites* sp. **I.** *Verrucosporites marginatus* (Mäder) Orłowska-Zwolińska. **J.** *Verrucosporites redactus* Orłowska-Zwolińska. **K.** *Conosmundasporites othmari* Klaus. **L.** *Anapiculatisporites telephorus* Pautsch. **M.** aff. *Acanthotriletes* sp. **N.** *Conbaculatisporites mesozoicus* Klaus. **O.** *Corrugatisporites scanicus* Nilsson. **P.** *Lycopodiumsporites rugulatus* (Couper) Schulz. **R.** *Lycopodiadicidites* cf. *kuepperi* Klaus. **S.** *Reticulatisporites* sp. **T.** aff. *Semiretisporis* sp. **U.** *Nevesisporites limatulus* Playford.

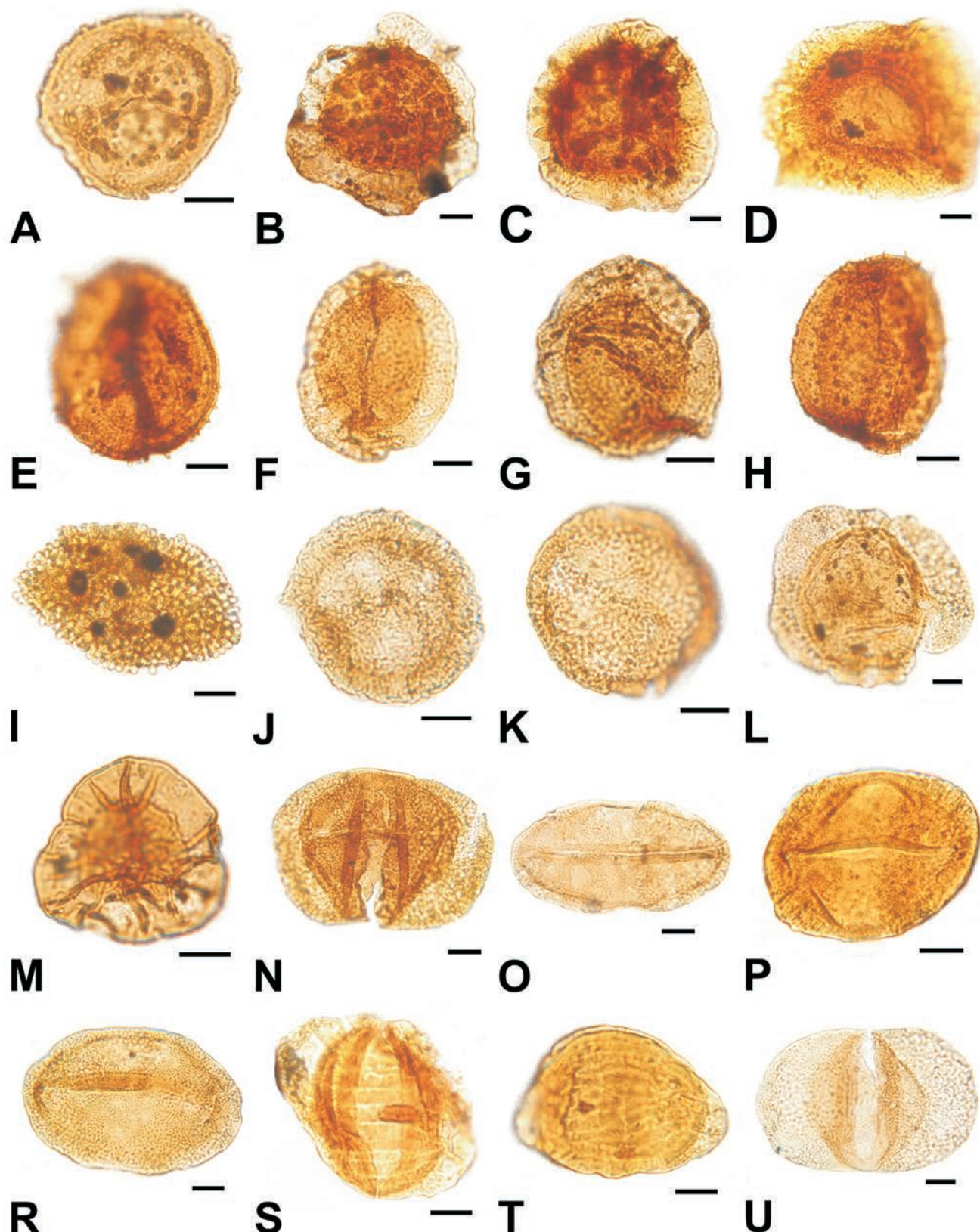


Fig. 9. Miospores from the Stuttgart Formation (Carmian), the Woźniki K1 borehole. Scale bar = 10 µm. A, J, N, U – depth 77.1 m; H, P, S, T – depth 77.7 m; A, K, M – depth 84.0 m; B–G, I, L, R – depth 84.45 m. **A.** aff. *Taurocuspites* sp. **B.** *Kraeuselisporites* cf. *cooksonae* (Klaus) Dettmann. **C.** *Kraeuselisporites lituus* (Leschik) Scheuring. **D.** *Kreuselisporites* sp. **E.** *Aratrisporites coryliseminis* Klaus. **F.** *Aratrisporites granulatus* (Klaus) Playford et Dettmann. **G, H.** *Aratrisporites paraspinosus* Klaus. **I.** *Retisulcites* sp. **J.** *Enzonalasporites manifestus* Leschik. **K.** *Enzonalasporites vigens* Leschik. **L.** *Accinctisporites* sp. **M.** aff. *Callialasporites* sp. **N.** *Illinites* cf. *chitonoides* Klaus alias *Succinctisporites grandior* Leschik sensu Mädler. **O.** *Ovalipollis lunensis* Klaus. **P.** *Ovalipollis* cf. *notabilis* Scheuring. **R.** *Ovalipollis ovalis* Krutzsch. **S.** *Protohaploxylinus* sp. **T.** *Striatoabietites aytugii* Visscher. **U.** *Parillintes* sp.

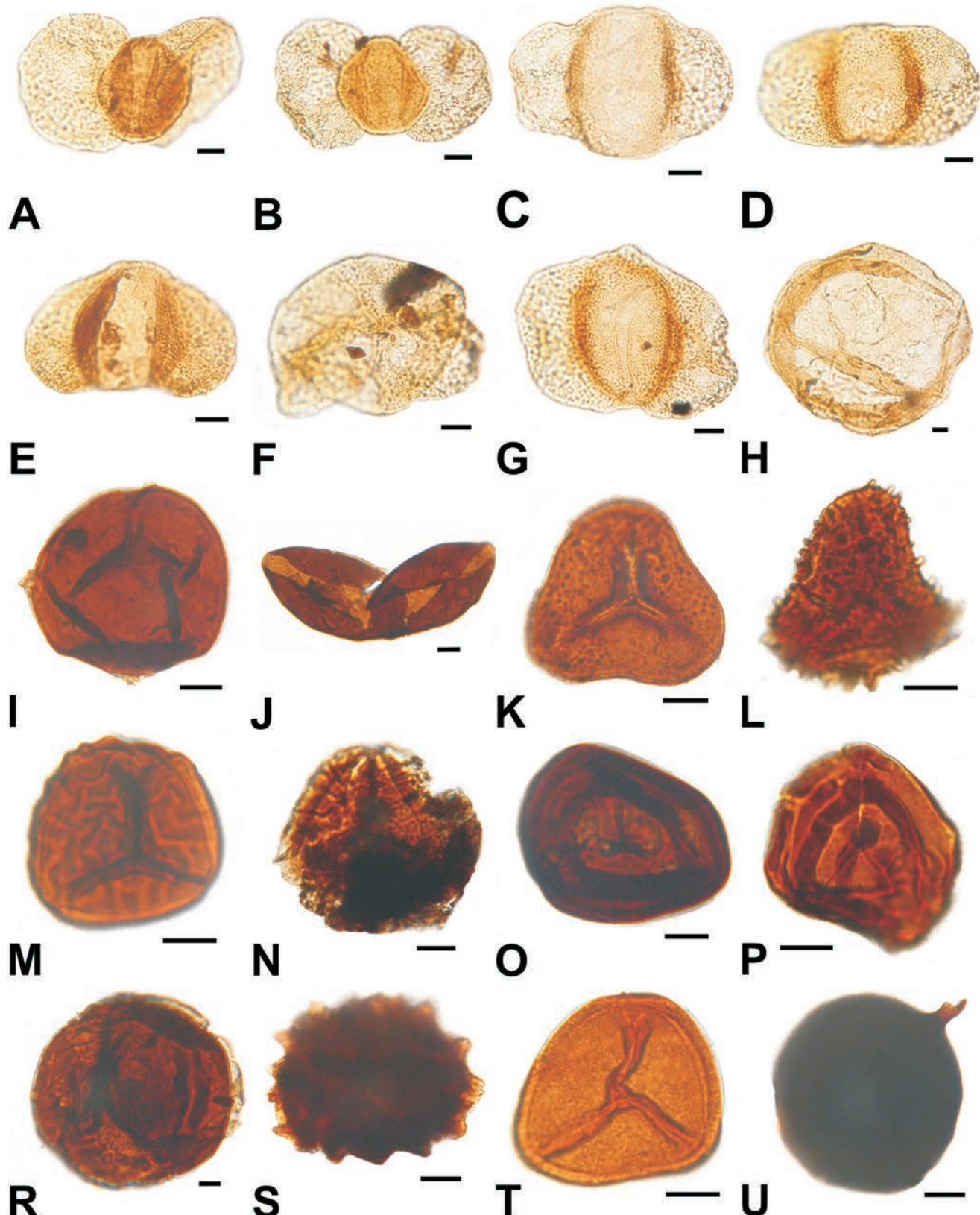


Fig. 10. Miospores from the Stuttgart Formation (Carnian), the Woźniki K1 borehole. Scale bar = 10 µm. I–S – stronger coalified and wasted forms; T–U – reworked forms. A, C, E, H–K, M – depth 77.1 m; L, O, S, U – depth 84.0 m; B, D, F, G, N, P.R, T – depth 84.45 m. **A.** *Platysaccus papilionis* Potonié et Klaus. **B.** *Platysaccus nitidus* Pautsch. **C.** *Alisporites* sp. **D.** *Triadispora polonica* Brugman. **E.** *Tradispora suspecta* Scheuring. **F.** *Triadispora* sp. **G.** *Labiisporites triassicus* Orłowska-Zwolińska. **H.** Alga *Schizosporis* sp. **I,** **J.** *Aulisporites astigmosus* (Leschik) Klaus. **K.** *Conbaculatisporites mesozoicus* Klaus. **L.** *Conbaculatisporites* sp. **M.** *Lycopodiacytidites kuepperi* Klaus. **N.** *Zebrasporites* sp. **O.** *Polycingulatisporites* sp. **P.** *Corrugatisporites* sp. **R,** **S.** Spore indet. **T.** *Densoisporites* sp. **U.** ?Chitinozoa.

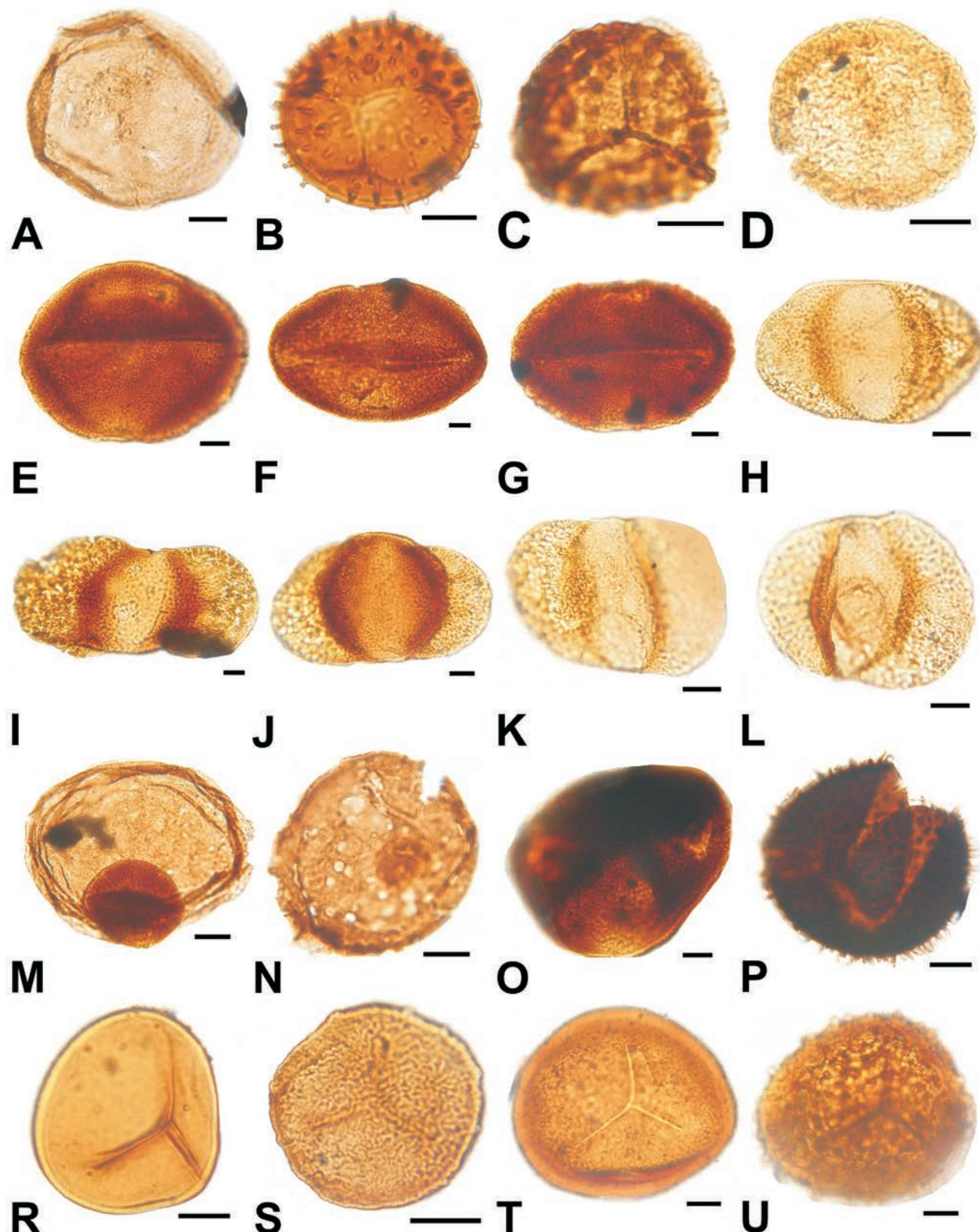


Fig. 11. Miospores from the Patoka Member (Norian) in the Patoka 1 borehole. Scale bar = 10 µm, except for M = 50 µm. B, E–H – stronger coalified forms; N–P – reworked forms. A, P – depth 199.0 m; S – depth 137.9 m; R, T, U – depth 153.1 m. **A.** *Calamospora* sp. **B.** *Anapiculatisporites telephorus* (Pautsch) Klaus. **C.** *Kraeuselisporites* sp. **D.** *Enzonalasporites manifestus* Leschik. **E.** *Ovalipollis rarus* Klaus. **F.**, **G.** *Ovalipollis ovalis* Krutzsch. **H.** *Alisporites toralis* (Leschik) Clarke. **I.** *Platysaccus* sp. **J.** *Triadispora crassa* Klaus. **K.** *Triadispora suspecta* Scheuring. **L.** *Triadispora* sp. **M.** Alga *Schizosporis* sp. **N.** *Calamospora* cf. *tener* (Leschik) de Jersey (degraded specimen). **O.** *Densoisporites neburgii* (Schulz) Balme. **P.** Spore indet. **R.** *Todisporites cinctus* (Maliavkina) Orlowska-Zwolińska. **S.** aff. *Conosmundasporites* sp. **T.** *Cyclotriletes* sp. **U.** *Baculatisporites* sp.

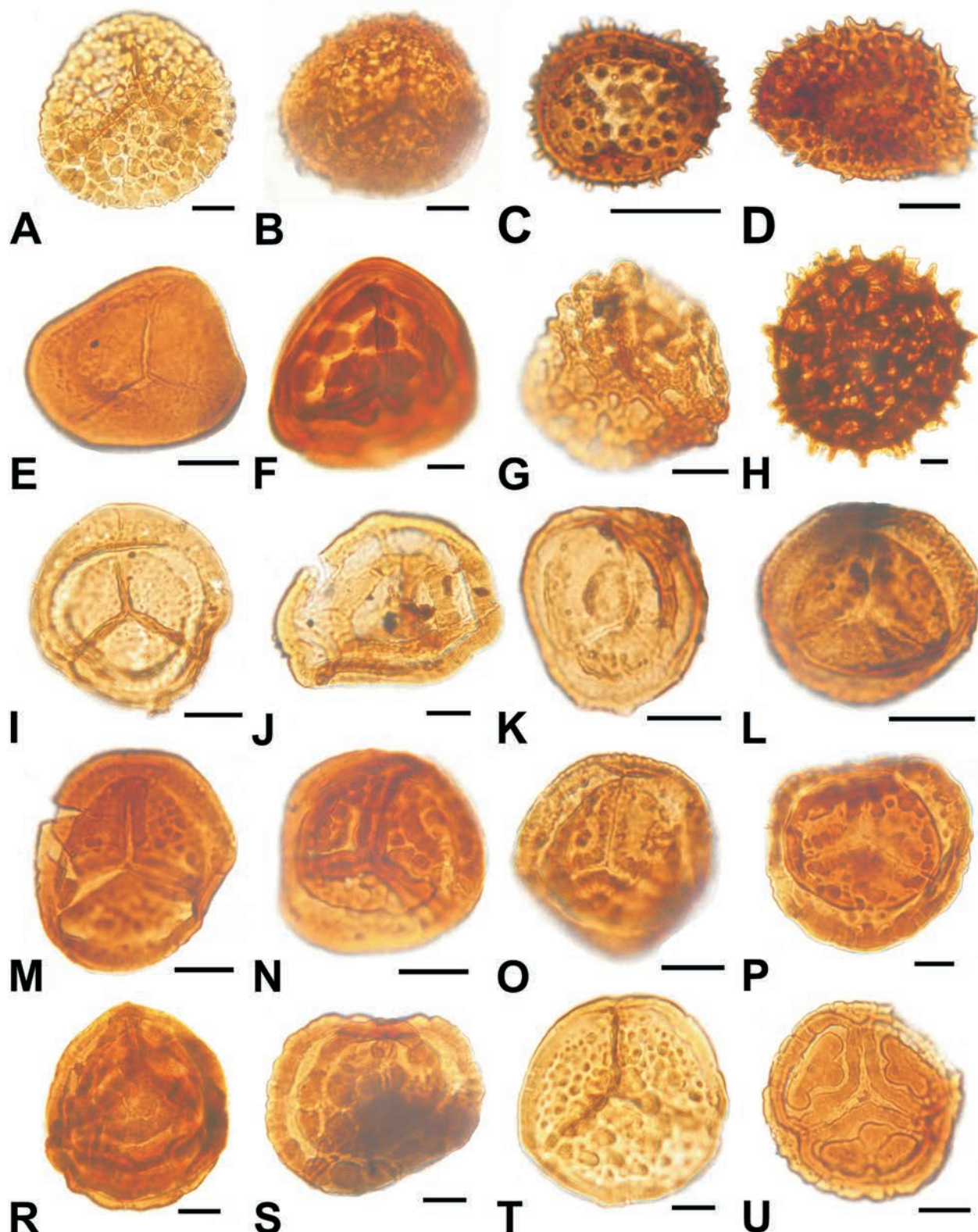


Fig. 12. Miospores from the Patoka Member (Norian) in the Patoka 1 borehole (A, B, D–S, U), Lipie Śląskie clay-pit (C) and Poręba outcrop (T). Scale bar = 10 µm, except C = 30 µm. L, N – depth 134.6 m; D, M, N, O – depth 137.9 m; B, E, F, G, R – depth 140.2 m; A, H–K, P, S, U – depth 153.1 m. **A.** *Verrucosisporites redactus* Orłowska-Zwolińska. **B.** *Porcellispora longdonensis* (Clarke) Scheuring. **C.** *Anapiculatisporites telephorus* (Pautsch) Klaus. **D.** *Anapiculatisporites spiniger* (Leschik) Reinhart. **E.** *Deltoidospora minor* Couper. **F.** *Corrugatisporites scanicus* Nilsson. **G.** *Foveolatiriletes* sp. **H.** *Reticulatisporites distinctus* Orłowska-Zwolińska. **I.** *Nevesisporites limatulus* Playford. **J.** *Neochomotriletes triangulatus* (Bolchovitina) Reinhart. **K.** *Polycingulatisporites reducens* (Bolchovitina) Playford et Dettmann. **L.** *Densosporites* sp. **M–O.** *Densosporites silesiensis* Fijałkowska-Mader sp. nov. **P.** *Densosporites rogalskai* Fijałkowska-Mader sp. nov. **R.** aff. *Polycingulatisporites* sp. **S.** *Taurocusporites cf. morbeyi* Orłowska-Zwolińska. **T.** *Taurocusporites verrucatus* Schulz. **U.** Spore sp. A.

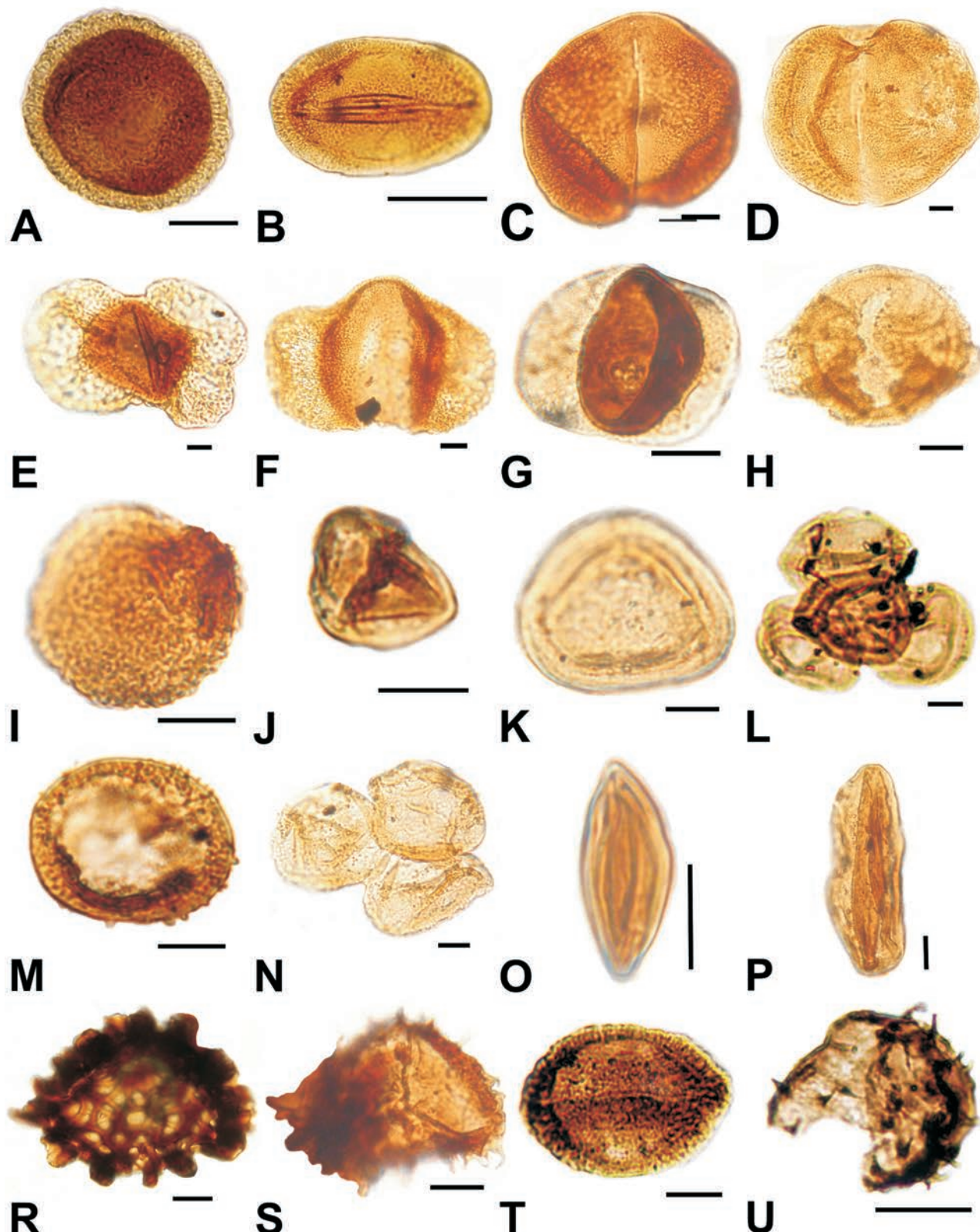


Fig. 13. Miospores from the Patoka Member (Norian) in the Patoka 1 borehole (C–H, N, P, T), Lipie Śląskie clay-pit (A, B, J, R) and Patoka clay-pit (I, K–M, O, S, U). Scale bar = 10 µm, except for A, B = 30 µm and R–T – stronger coalified and degraded forms; U – re-worked form. C, F, G, P – depth 137.9 m; D, N – depth 140.2 m; E, H, T – depth 153.1 m. **A.** *Enzonalasporites vigens* Leschik. **B.** *Ovalipollis ovalis* Krutzsch. **C.** *Brachysaccus neomundanus* (Leschik) Mädler. **D.** *Parillinites* sp. **E.** *Platysaccus niger* Mädler. **F.** *Falcisporites* sp. **G.** *Labiisporites triassicus* Orłowska-Zwolińska. **H.** *Protodiploxylinus* sp. **I.** *Partitisporites* sp. **J.** *Duplicisporites granulatus* Leschik. **K.** *Classopollis meyeriana* (Klaus) de Jersey. **L.** *Classopollis meyeriana* (Klaus) de Jersey (tetrade). **M.** *Granuloperculatipollis rufid* Venkatachala et Goczán. **N.** *Granuloperculatipollis rufid* Venkatachala et Goczán (tetrade). **O.** *Monsulcites minimus* Cookson. **P.** *Monosulcites* sp. **R.** *Reticulatisporites* sp. **S.** aff. *Kraeuselisporites* sp. **T.** *Ovalipollis ovalis* Krutzsch. **U.** Acritarcha indet.

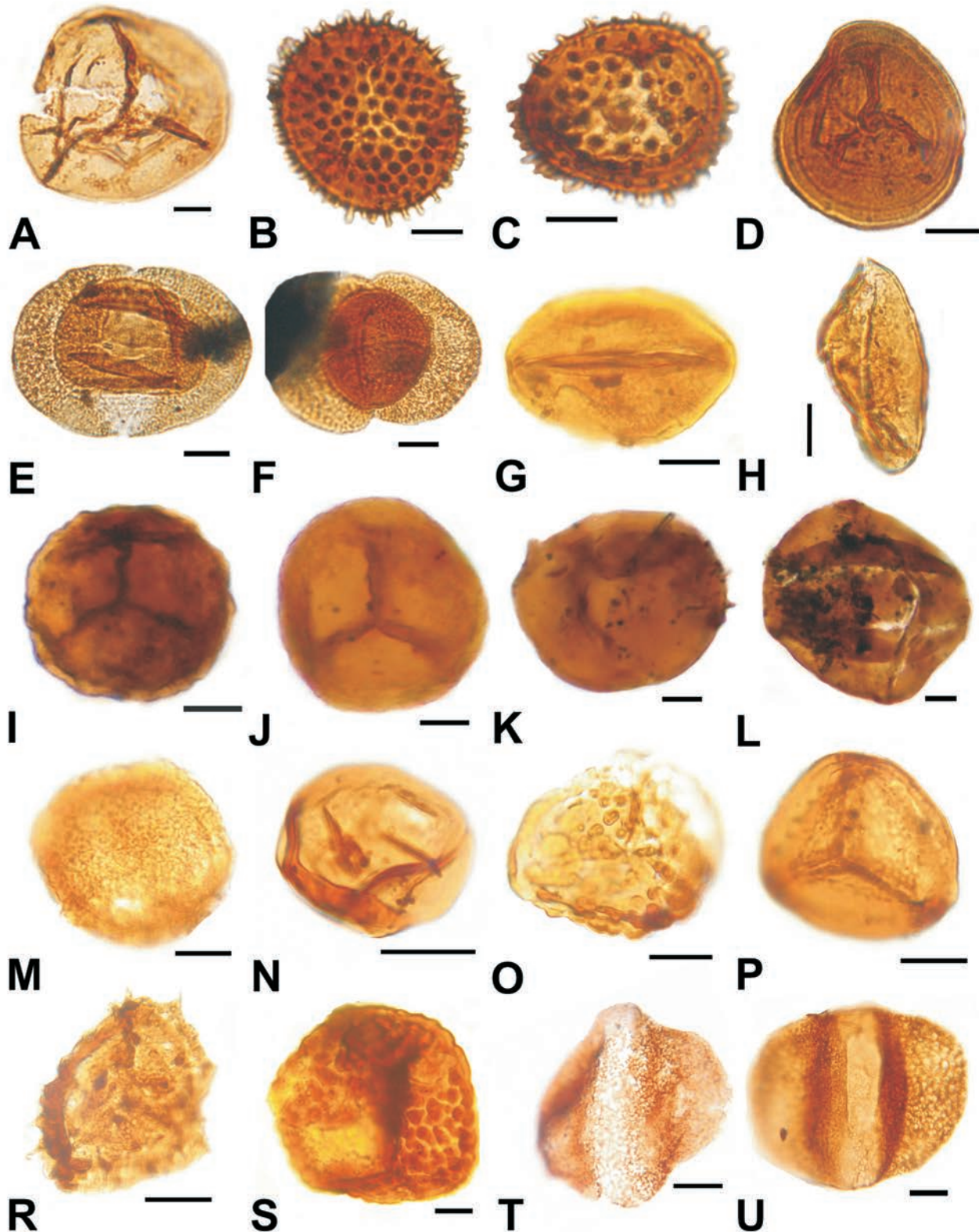


Fig. 14. Miospores from the upper part of the Patoka Member (Norian) in the Kobylarz 1 borehole (A–L) and from the “Połomia Formation” (?Rhaetian) (M–O), the upper part of the Patoka Member (P–S) and the lower part of the Patoka Member (T–U), Patoka 1 borehole. Scale bar = 10 µm. I, J, K – reworked forms. A–C – depth 7.5 m; D–L – depth 8.0 m; M–O – depth 18.1 m; P–S – depth 35.7 m; T, U – depth 116.7 m. **A.** aff. *Todisporites* sp. **B.** *Anapiculatisporites spiniger* (Leschik) Reinhardt. **C.** *Anapiculatisporites telephorus* (Pautsch) Klaus. **D.** *Densosporites* sp. **E.**, **F.** *Lunatisporites* sp. **G.** *Ovalipollis* sp. **H.** aff. *Monosulcites* sp. **I.** *Densoisporites playfordii* (Balme) Dettmann. **J.** *Densoisporites* cf. *playfordii* (Balme) Dettmann. **K.** aff. *Punctatisporites* sp. **L.** *Lunatisporites* sp. (degraded specimen). **M.** aff. *Accinctisporites* sp. **N.** *Calamospora* sp. **O.** *Taurocusporites verrucatus* Schulz. **P.** *Densosporites* sp. **R.** *Kraeuselisporites* sp. **S.** *Verrucosporites* sp. **T.** *Falcisporites* sp. **U.** *Alisporites toralis* (Leschik) Clarke.

lipollis (Fig. 14G), *Parillinites* and *Brachysaccus*, whereas the pollen *Lunatisporites* (Fig. 14E, F) and *Cedripites* occurred less frequently. The lycopsid spores *Anapiculatisporites* (Fig. 14B, C) and *Densosporites* are rare. Fern spores aff. *Todisporites* (Fig. 14A) and the pollen of cycads were infrequent. The assemblage was further characterized by a high content of reworked early Triassic miospores, mainly *Densoisporites* (Fig. 14I, J) accompanied by strongly degraded, undeterminable spores and pollen grains.

Three miospore assemblages were identified in the Patoka 1 borehole (Figs 4, 5):

- the assemblage at a depth of 17.4–18.1 m, within the kaolinite interval of the “Połomia Fm”, consists of single occurrences of the spores *Calamospora* (Fig. 14N), *Taurocusporites* (Fig. 14O), *Todisporites*, *Densosporites* and *Camazonosporites*, as well as the monosaccate pollen aff. *Accinctisporites* sp. (Fig. 14M) and bisaccate pollen of the genera *Ovalipollis*, *Lunatisporites* and *Triadispora*;

- the assemblage at 35.7–36.6 m, near the erosional top of the Patoka Mbr in this section, contains the same taxa as described in the assemblage above at 17.4–18.1 m (Fig. 14P) and also *Enzonalasporites*, *Falcisporites* (Fig. 14T) and *Alisporites* (Fig. 14U), as well as spores of the genera *Kraeuselisporites* (Fig. 14R) and *Verrucosisporites* (Fig. 14S). In addition, the alga *Schizosporis* and undeterminable, degraded spores also occur in the assemblage;

- the assemblage at 116.70–118.50 m, in the middle part of the Patoka Mbr (in the bone-bearing horizon), consists mainly of conifer pollen, assigned to *Ovalipollis*, *Brachysaccus*, *Parillinites*, *Alisporites* and *Triadispora*. Other pollen *Striatoabietites*, *Platysaccusand*, *Falcisporites* and the spores of *Verrucosisporites*, *Todisporites*, *Cyclotriletes*, *Densosporites* and *Corrugatisporites* are rare and occur only as single specimens. Reworked early Triassic and probably older spores are relatively abundant.

PALYNOSTRATIGRAPHY

Three palynological zones were recognized in the Upper Triassic deposits of Upper Silesia: longdonensis within the “Chrzanów Fm”, astigmosus in the Stuttgart Fm and meyeriana in the Patoka Mbr of the Grabowa Fm (Figs 5, 15). The miospore assemblages found in the “Chrzanów Fm” represent the verrucata Subzone, whereas those in Patoka Mbr belong to the meyeriana b Subzone.

Age of the Lisowice bone-bearing horizon

The stratigraphical position of the Patoka Mbr interval, containing the Lisowice bone-bearing horizon (*sensu* Szulc and Racki, 2015; Fig. 2), is the most controversial matter in the Upper Silesian Keuper (see Szulc *et al.*, 2015). The first determination of the early Rhaetian age of the megaspore assemblage from the Lipie Śląskie clay-pit by Fuglewicz and Śnieżek (1980) was questioned by Marcinkiewicz (1981). The spectrum under discussion contains the two species *Radosporites planus* (Reinhardt et Fricke) Kozur and *Horstisporites imperfectus* Reinhardt et Fricke, the stratigraphical range of which is limited to the Stuttgart Fm

CHRONOSTRATIGRAPHY		LITHOSTRATIGRAPHY (Becker <i>et al.</i> , 2008; Szulc and Racki, 2015)	PALYNOSTRATIGRAPHY	
			Zones	Subzones
TRIASSIC	CARNIAN NORIAN	KEUPER GROUP Grabowa Fm	Woźniki Mbr	
			Patoka Mbr	meyeriana b
			Ozimek Mbr	
			Stuttgart Fm	astigmosus
			“Chrzanów Fm”	longdonensis verrucata

Fig. 15. Palynostratigraphy of the Upper Triassic in Upper Silesia region.

of Carnian age. The assignation of an early Rhaetian age to *Hostisporites bertelsenii* Fuglewicz on the basis of similarity to *Horstisporites* sp. is also doubtful. In addition, the index species *Trileites pinguis* (Harris) Potonié was determined as conformis. The occurrence of the species *T. pinguis* itself does not determine the Rhaetian age of the megaspore assemblage described by Fuglewicz and Śnieżek (1980), as the pinguis Zone corresponds to the late Norian and Rhaetian (see Marcinkiewicz *et al.*, 2014). In support of a Rhaetian age is the presence of such megaspore species as *Tasmanitriletes pedinacron* (Haris) Jux et Kempf, *Verrutriletes utilis* (Marcinkiewicz) Marcinkiewicz and *V. litchii* (Harris) Potonié, which have not been reported from this assemblage.

Next, Heunisch recognized the miospore meyeriana b Subzone in the Patoka Mbr at four localities, the Lipie Śląskie clay-pit, the Czarny Las borehole, and the Poręba and Zawiercie outcrops (partly published in Szulc *et al.*, 2006; Fig. 5). The same meyeriana b Subzone was identified by Stanczko (2007) in the Lipie Śląskie clay-pit. The inventory of miospores by this author generally concurs with the palynological data obtained by Heunisch (in Szulc *et al.*, 2006) and Fijałkowska-Mader (this paper), excluding the occurrence of *Riccisporites tuberculatus*. Neither Heunisch nor Fijałkowska-Mader found it in the spectra analyzed (with the exception of the single specimen from the Woźniki borehole, at a depth of 30 m). In addition, the photograph of the miospore presented by Stanczko (plate 1, fig. 4) is of such poor quality that the correctness of the identification of this guide species is questionable.

In the papers of Dzik *et al.* (2008a, b), concerning the bone-bearing strata in the Lipie Śląskie clay-pit, two miospore species of suggested Rhaetian age, *Brachysaccus neomundanus* and *Monosulcites minimus*, were mentioned. *B. neomundanus* is known in spore-pollen spectra occurring since the Ladinian, so combining it with the Rhaetian conifer *Stachyotaxis* is rather doubtful. The single gingkolean pollen *Monosulcites minimus* appears already in the late Norian.

The palynozonal aspect of the Upper Triassic in the Lipie Śląskie section was again raised recently by Pieńkowski *et al.* (2014). The authors, with reference to new miospore determinations quoted in Świło *et al.* (2014),

made reference to only the meyeriana c Subzone and the higher tuberculatus Zone. In the description of the miospore assemblage from the Lipie Śląskie clay pit given by Świło *et al.* (2014), the taxon *Rhaetipollis germanicus* admittedly was noted, but without any illustration. Moreover, there is no information about the frequency of specimens (so important in this case), that essentially influenced the credibility of the determination of the age as meyeriana c Subzone – tuberculatus Zone (the latest Norian–Rhaetian).

An important contribution to a solution for the problem of the age of the deposits at the Lipie Śląskie locality could be the palynological studies of the adjacent boreholes and outcrops, containing the same characteristic Lisowice bone-bearing horizon, carried out by Heunisch (in Szulc *et al.*, 2006), Wawrzyniak (in Sadlok and Wawrzyniak, 2013) and Fijałkowska-Mader (this paper). Assemblages of the meyeriana b Subzone were found in two boreholes, Patoka 1 (134.6–153.1 m) and Poręba (7.7–11.4 m) as well as in the Poręba and Zawiercie outcrops (the latter correlated with the Lipie Śląskie locality by Niedźwiedzki *et al.*, 2014).

In conclusion, there is no clear palynological evidence, either for the correlation of the Lisowice bone-bearing horizon with the meyeriana c Subzone, or for the Rhaetian age of this succession.

Degraded and reworked palynomorphs

The relatively large amount of degraded and reworked forms in the assemblages from the Patoka Mbr hinders the determination of its age. The most common are the early Triassic spores *Densoisporites* (Figs 10T, 11O, 14I, J). Single specimens of the spores assigned to the early Triassic genera *Palyfordinaspora* and *Punctatisporites* were also found. Moreover, the Anisian spores *Perotrilites minor* and a form resembling the Palaeozoic chitinozoans (Fig. 10U), and undetermined acritarchs (Fig. 13U) were found as well.

The co-occurrence of palynomorphs so heterochronous in the material studied confirms the intensive recycling phenomena recorded in the middle Keuper strata and may evidence the repeated cannibalistic redeposition of it (see e.g., Bilan 1976, Szulc and Racki, 2015).

PALYNOFACIES ANALYSIS

The definition of Powell *et al.* (1990) was applied for palynofacies: “a distinctive assemblage of palynoclasts whose composition reflects a particular sedimentary environment”. The following organic matter particles (palynoclasts), classified after APOMC (Amsterdam Palynological Organic Matter Classification) '93 (Anonymous, 1993), occur as four groups in the studied material:

- palynomorphs – spores, pollen, prasinophytes, chlorococcales, dinocysts, acritarchs, fungal spores;
- structured organic matter – wood, cuticles, degraded organic matter (DOM);
- unstructured/amorphous organic matter (AOM; to avoid the misunderstanding, this is not amorphous matter sensu Boulter and Riddick, 1986) – homogeneous particles (particles 1–2 µm with well-defined outline and uniform ap-

pearance), heterogeneous particles (non-homogeneous particles 1–2 µm with well-defined outlines), finely dispersed matter (all particles 1–2 µm);

- indeterminate organic matter.

On the basis of the percent ratio of the particular palynoclasts groups, four types of palynofacies have been distinguished (Figs 16–18).

Type 1

Characteristics: Palynomorphs are absent, wood reaches 0–20%, DOM 5%, AOM (80–100%) is dominated by finely dispersed matter; black, opaque organic particles predominate (Fig. 18A).

Occurrence: Within the coarse- and variable-grained sandstones with large-scale cross-bedding, making up simple sedimentary cycles, which locally begin with a river-bed pavement [Patoka 1 borehole at 23.70 m (“Połomia Fm”), 66.40 m, 75.00 m, 81.20 m, 85.80 m, 93.50 m, 110.40 m, 113.40 m, 150.00 m, 158.90 m and 159.10 m (Patoka Mbr; Fig. 16), and Woźniki K1 borehole at 68.80 and 79.50 m (Stuttgart Fm; Fig. 17)].

Depositional environment: Sedimentary structures and strong degradation of the palynoclasts indicate high-energy conditions, which occur in the fluvial channels of braided rivers (e.g., Fijałkowska, 1994; Tyson, 1995, p. 213).

Type 2

Characteristics: Palynomorphs, mainly pollen grains, reach 0–5%, wood – 5–15%, cuticles 1%, DOM – 2–10%, AOM (70–90%) consists of finely dispersed and heterogeneous matter; black, opaque organic particles predominate (Fig. 18B).

Occurrence: In the structureless sandy mudstones of the Patoka Mbr (Patoka 1 borehole at 114.70 m, 115.50 m and 116.70 m; Fig. 16).

Depositional environment: The character of the deposits and the palynoclasts indicates lower-energy conditions (by comparison with a fluvial channel) of the floodplain (e.g., Fijałkowska-Mader *et al.*, 2015).

Type 3

Characteristics: Spores reach 10–50% in the proximal facies and several to 10% in the distal facies, pollen – several to 50% in the proximal facies and to 50–70% in the distal facies, fresh-water algae and fungal spores – less than 1%; wood – several to 40%, cuticles relatively abundant increase up to 20% in the proximal facies and several percent in the distal facies; AOM 10–50% is dominated by heterogeneous matter in the proximal facies and finely dispersed in the distal facies; black, opaque organic particles reach on average 50–60%, dark-brown, translucent – 5–10%, light brown and yellow – 10–25% (Fig. 18C–E).

Occurrence: In the structureless siltstones of the “Połomia Fm” (Patoka 1 borehole at 17.40 m and 18.10 m); in the siltstones and mudstones with small-scale cross-lamination (Patoka 1 borehole at 35.70 m, 36.60 m, 134.60 m, 137.90 m and 140.20 m); in the horizontal-laminated mudstones (Patoka 1 borehole at 145.10 m); in the structureless mudstones (Patoka 1 borehole at 199.0 m (Patoka Mbr; Fig. 16), Patoka clay-pit, Lipie Śląskie clay-pit, Poręba outcrop; Woźniki K1 borehole at 77.10 m, 77.70 m, 82.50 m, 84.00 m and

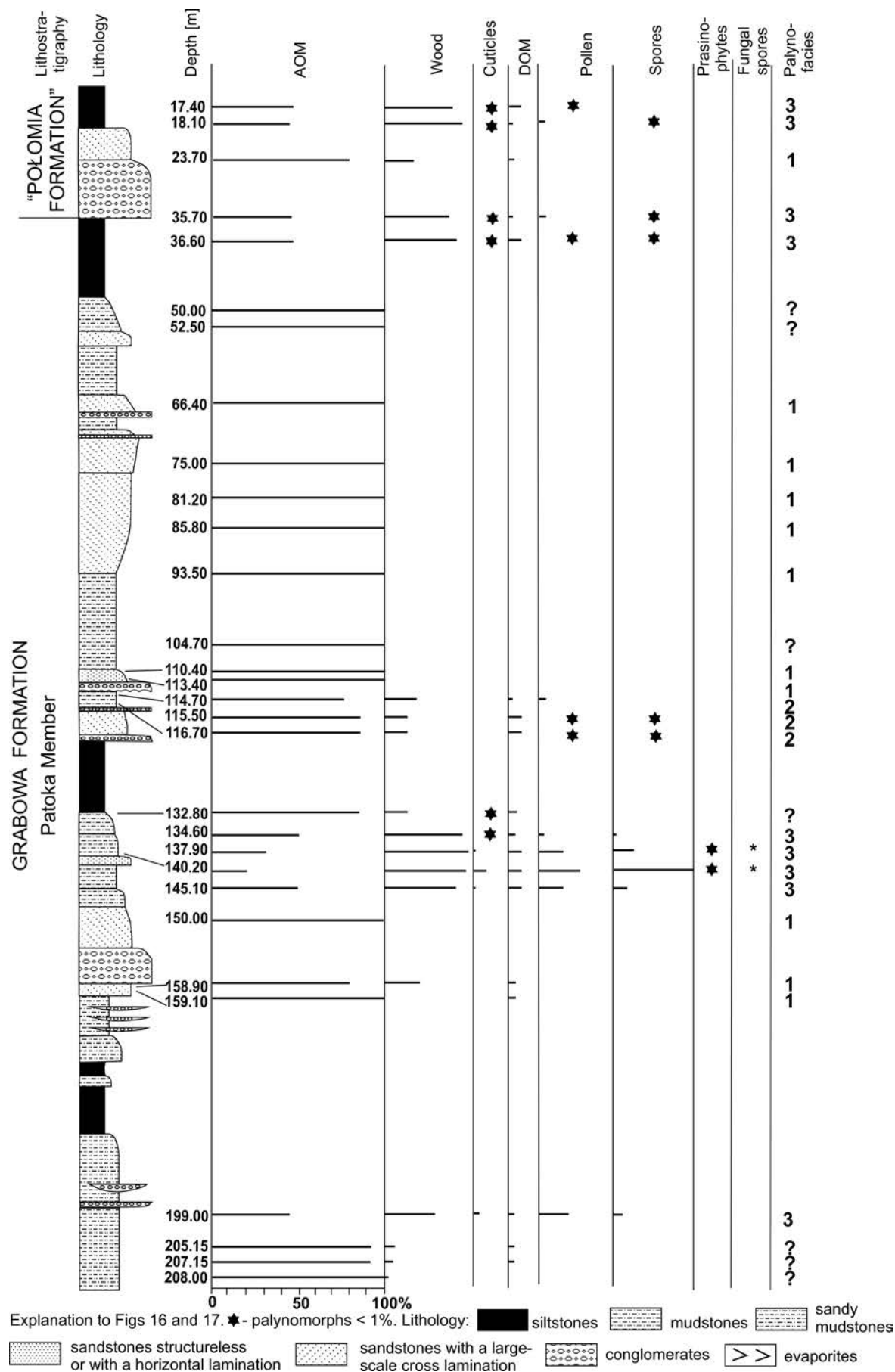


Fig. 16. Palynofacies analysis of the Upper Triassic deposits in the Patoka 1 borehole.

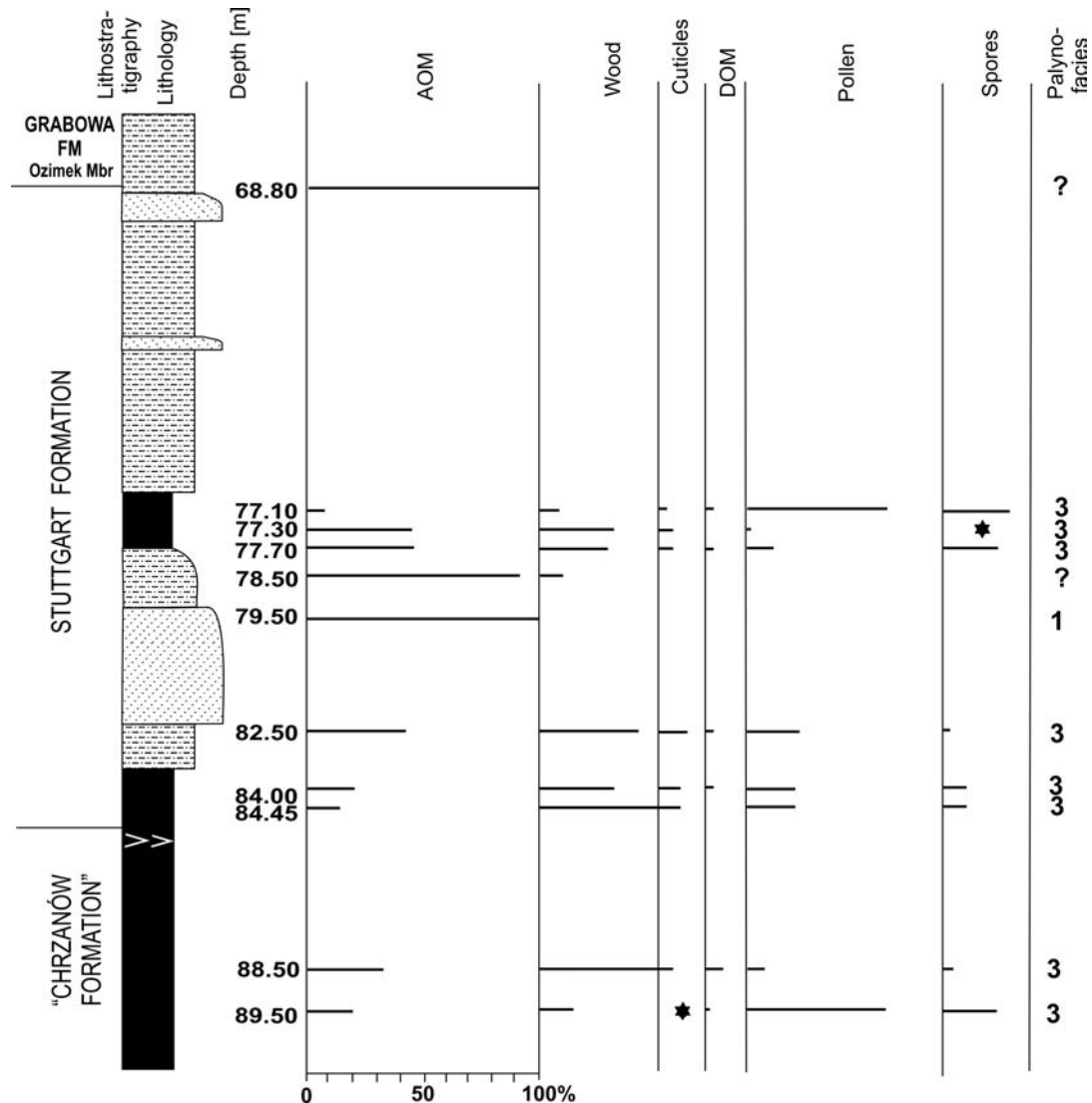


Fig. 17. Palynofacies analysis of the Upper Triassic deposits in the Woźniki K1 borehole. For explanations see Fig. 16

84.45 m (Stuttgart Fm), 88.50 and 89.50 m (“Chrzanów Fm”; Fig. 17).

Depositional environment: A large amount of spores, cuticles and wood as well as the presence of fresh-water algae are characteristic for a freshwater lacustrine basin (e.g., Heunisch, 1990; Van Bergen and Kerp, 1990; Boulter, 1994, fig. 11.2; Fijałkowska, 1994; Pieńkowski and Waksmundzka, 2009; Heunisch *et al.*, 2010; Fijałkowska-Mader *et al.*, 2015). The two samples from the evaporite-bearing “Chrzanów Fm” could represent a playa basin (e.g., Hauenschke and Heunisch, 1989, 1990; Fijałkowska, 1994; Fijałkowska-Mader, 2011; Fijałkowska-Mader *et al.*, 2015).

Type 4

Characteristics: Palynomorphs are absent, wood fragments reach 0–10%, AOM 90–100%, including heterogeneous, homogeneous and finely dispersed matter; black, opaque, organic particles 90–100% (Fig. 18F).

Occurrence: Within the structureless or streaky, laminated mudstones (Patoka 1 borehole at 50.00 m, 52.50 m, 104.70 m, 132.80 m, 205.15 m, 207.15 m and 208.00 m (Patoka Mbr;

Fig. 16) and Woźniki K1 borehole at 68.80 m (Stuttgart Fm; Fig. 17).

Depositional environment: undetermined.

PALAEOENVIRONMENTAL AND PALAEOCЛИMATIC INTERPRETATION

The palynofacies analysis confirms the earlier suggestions that the “Chrzanów Fm” was deposited in a playa basin (see Bilan, 1976; Deczkowski, 1997; Fig. 19).

The composition of the miospore assemblage, occurring in this formation, consisting most exclusively of conifer pollen with numerous *Triadispora* specimens, indicates a very dry climate in the early Carnian (see Orłowska-Zwolińska, 1983; Ziegler *et al.*, 1994). Both conifers *Voltzia* and *Albertia* producing the *Triadispora* pollen and lycopsids *Lycostrobus* and *Annalepis*, the parent plants of the spore *Aratrisporites* (see Grauvogel-Stamm, 1969; Orłowska-Zwolińska, 1979), also are known from settings of higher salinity (Mader, 1990, 1997).

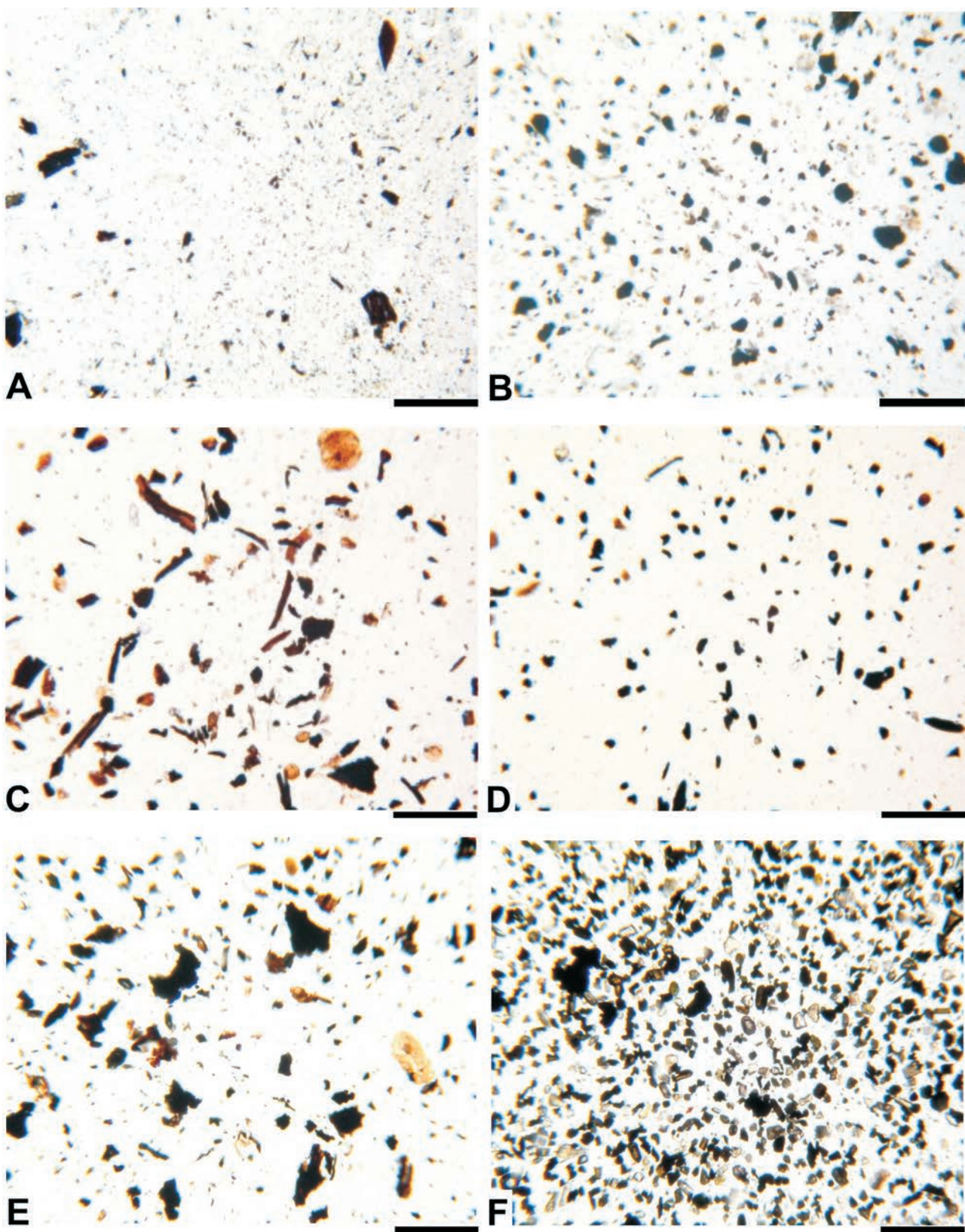


Fig. 18. Types of palynofacies from the Patoka Member (Norian) in the Patoka 1 borehole (A, D, F), the Kobylarz 1 borehole (B), Stuttgart Formation (Carnian) in the Woźniki K1 borehole (C) and “Chrzanów Formation” (Carnian) in the Woźniki K1 borehole (E). A – depth 113.4 m; B – depth 9.0 m; C – depth 84.0 m; D – depth 36.6 m; E – depth 89.5 m; F – depth 205.15 m. A, C–F – scale bar 200 µm, B – scale bar 150 µm. **A.** Palynofacies 1; fluvial environment – fluvial channels. **B.** Palynofacies 2; fluvial environment – floodplain. **C.** Palynofacies 3; lacustrine environment, proximal zone. **D.** Palynofacies 3; lacustrine environment, distal zone. **E.** Palynofacies 3; playa environment, proximal zone. **F.** Palynofacies 4; undetermined environment.

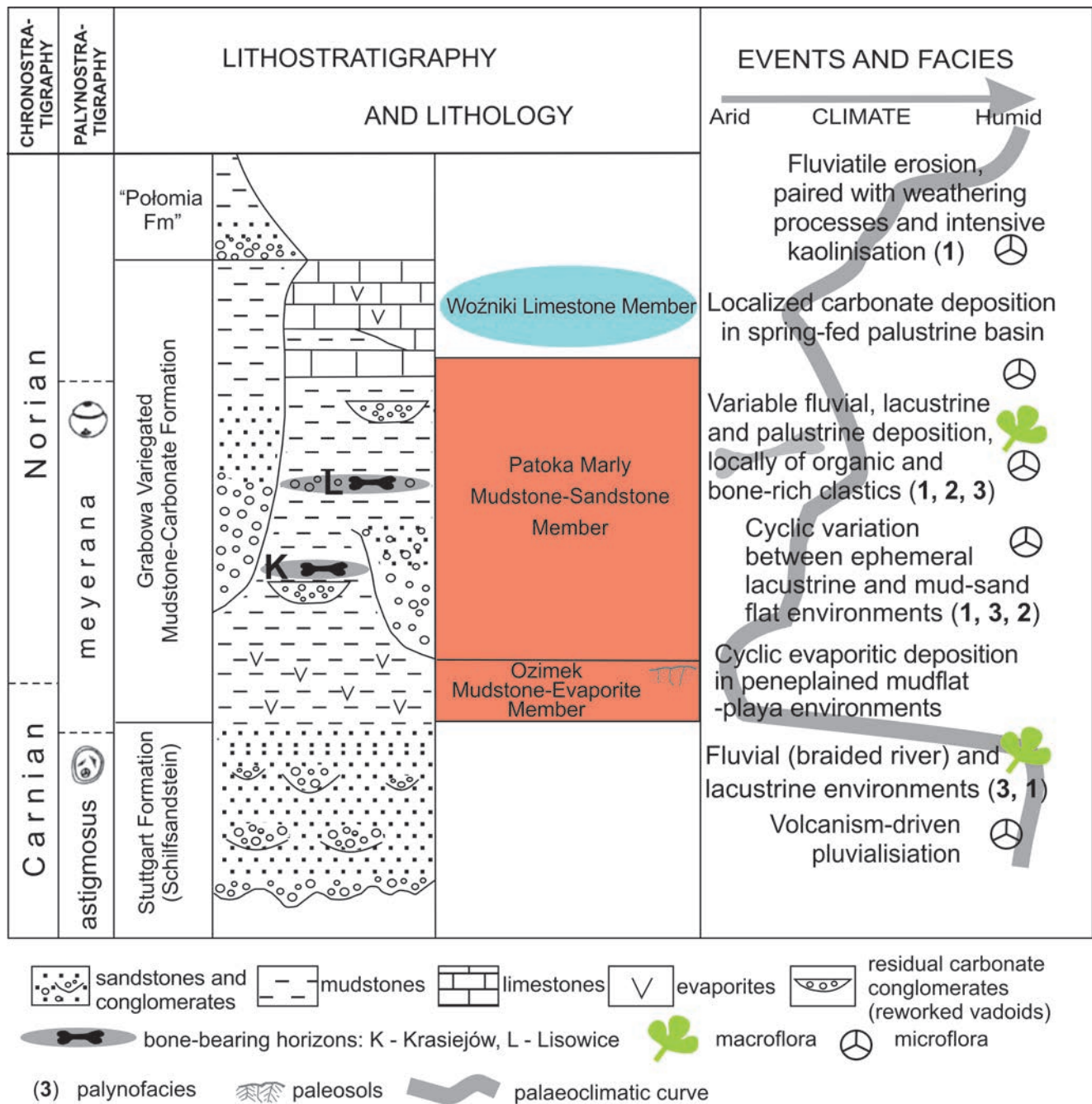


Fig. 19. Stratigraphy-facies and scheme of climate-driven sedimentation events of the middle and upper Keuper of Upper Silesia, to show the new formal lithostratigraphic unit (Grabowa Formation and subordinate units) and temporal relationships between the two bone-bearing horizons under study (after Fig. 9 in Szulc and Racki, 2015); the microflora numbers correspond to palynofacies types (see Fig. 18).

The palynofacies occurring in the Stuttgart Fm are characteristic for fluvial and lacustrine milieu and consistent with the sedimentological interpretation (see Deczkowski, 1977). This environmental interpretation may be confirmed by abundant spores *Aulisporites astigmosus*, produced most probably by plants, which overgrew the river floodplains (e.g., Orłowska-Zwolińska, 1983). The miospore assemblage, dominated by equisetaleans (*Sphaenopsida*), fern spores of the Osmundaceae and Mariatiaceae families and lycopsid spores, indicates a humid climate in the middle Carnian (Julian). An increase in precipitation – the “Car-

nian Pluvial Event” – could be connected with volcanic activity in the Wrangellia and/or Eastern Mediterranean areas (e.g., Kozur and Bachman, 2010; Roghi *et al.*, 2010; Dal Corso *et al.*, 2012; Arche and López-Gómez, 2014; Fig. 19).

The deposition of the evaporite-bearing Ozimek Mbr (lower part of the Grabowa Fm) took place in a peneplained mudflat-playa basin in dry climatic conditions (Szulc and Racki, 2015). The Patoka Mbr (middle-upper part of the Grabowa Fm) was formed in a wide spectrum of environments: fluvial, lacustrine, palustrine and mud-sand flat (Środoń *et al.*, 2014; Szulc and Racki, 2015). Both the char-

acter of sediments and the higher ratio of hygrophytic elements (lycopsisid and equisetalean spores) in the miospore spectra indicate that the humidification of climatic conditions was connected with a pluvial event, which occurred in the middle-late Norian (Berra *et al.*, 2010; Preto *et al.*, 2010; Fig. 19). According to Vakhrameev (1981, 1987, 1991), a high frequency of the pollen Classopolis is evidence of a warm climate.

The “Połomia Fm” was deposited in fluvial environments (e.g., Szulc *et al.*, 2006; Pieńkowski *et al.*, 2014; Środoń *et al.*, 2014; Szulc and Racki, 2015) and may be connected with the pluvialisation of climate in the Rhaetian (e.g., Michalík *et al.*, 2010; Preto *et al.*, 2010; Brański, 2011; Haas *et al.*, 2012; Lintnerová *et al.*, 2013; Pieńkowski *et al.*, 2014; Szulc and Racki, 2015), even if the available palynostratigraphic dating remains equivocal.

CONCLUSIONS

1. The miospore assemblage occurring in the “Chrzanów Fm” in the Woźniki K1 borehole represents the Carnian verrucata Subzone of the longdonensis palynological Zone.

2. The miospore assemblage recognized in the Stuttgart Fm in the Woźniki K1 borehole represents the Carnian astigmosus palynological Zone.

3. Presentation of the detailed palynostratigraphy of the Grabowa Fm is difficult, owing to the poor state of miospore preservation and redeposition phenomena, recorded in the sections studied. In the majority of the analyzed samples from the Patoka Mbr (also from the Lisowice bone-bearing horizon in the Lipie Śląskie clay-pit and the Zawiercie outcrop), miospore assemblages represent the middle Norian meyeriana b Subzone.

4. The Rhaetian age of the Grabowa Fm in the Lisowice–Lipie Śląskie clay-pit suggested in the literature is not reliably documented, as the index Rhaetian miospore species were never illustrated.

5. The results of palynofacies analysis confirm earlier environmental interpretations, based on sedimentological premises and the analysis of clay minerals (Środoń *et al.*, 2014; Szulc *et al.*, 2015), in which the “Połomia Fm” was deposited in fluvial environments, the Patoka Mbr in variable fluvial and lacustrine milieu, the Stuttgart Fm in fluvial and lacustrine environments, and the “Chrzanów Fm” in a playa basin.

6. Changes in the composition of the miospore assemblages reflect changes in the palaeoclimate from dry conditions in the early Carnian, through the “Carnian Pluvial Event” in the Julian and aridization of climate at the Carnian/Norian boundary to the mid-late Norian pluvial event. Mostly coarse-grained deposition of the “Połomia Fm” could be connected with the pluvial conditions that occurred in the Rhaetian.

Acknowledgments

Authors thank Bas van de Schootbrugge for help with the determination of miospores from the Patoka clay-pit and Paweł Filii-

piak for preparation and photographic documentation of one sample from the Patoka clay-pit. The manuscript benefited greatly from the remarks and comments of Simonetta Cirilli and Sofie Lindström. Financial support for this study was provided by the Polish Ministry of Science and Higher Education (Grant N30711 7037 to G. Racki).

REFERENCES

- Anonymous, 1993. Amsterdam Palynological Organic Matter Classification, *Open Workshop Materials, Oct. 29th – Nov. 1st, 1993*. Louisiana Universities Marine Consortium, Cocodrie, pp. 6.
- Arche, A. & López-Gómez, J., 2014. The Carnian Pluvial Event in West Europe: new data from Iberia and correlation with the Western Neotethys and Eastern North America-NW Africa regions. *Earth-Sciences Reviews*, 128: 196–231.
- Becker, A., Kuleta, M., Narkiewicz, K., Pieńkowski, G. & Szulc, J., 2008. Trias. In: Wagner, R. (ed.), *Tabela stratygraficzna Polski, Polska pozakarpacka*. Państwowy Instytut Geologiczny, Warszawa. [In Polish.]
- Berra, F., Jadoul, F. & Anelli, A., 2010. Environmental control on the end of the Dolomia Principle/Hauptdolomit depositional system in the central Alps: Coupling sea-level and climatic changes. *Palaeogeography, Palaeoclimatology, Palaeoecology*, 290: 138–150.
- Bilan, W., 1976. The stratigraphy of the Upper Triassic deposits of the eastern margin of the Upper Silesian Coal Basin. *Zeszyty Naukowe AGH, Geologia*, 2 (3): 4–73. [In Polish, with English summary.]
- Boulter, M. C., 1994. An approach to a standard terminology for palynodebris. In: Traverse, A. (ed.), *Sedimentation of Organic Particles*. Cambridge University Press, Cambridge, pp. 199–216.
- Boulter, M. C. & Riddick, A., 1986. Classification and analysis of palynodebris from the Palaeocene sediments of the Forties Field. *Sedimentology*, 33: 871–886.
- Brański, P., 2011. Clay mineral composition in the Triassic and Jurassic deposits from the Polish Basin – a record of palaeoclimatic and palaeoenvironmental changes. *Biuletyn Państwowego Instytutu Geologicznego*, 444: 15–32. [In Polish, with English summary.]
- Cirilli, S., 2010. Upper Triassic-lowermost Jurassic palynology and palynostratigraphy: a review. In: Lucas, S. G. (ed.), *The Triassic Timescale. Geological Society of London Special Publication*, 334: 221–262.
- Dal Corso, J., Mietto, P., Newton, R., J., Pancost, R., D., Preto, N., Roghi, G. & Wignall, P., 2012. Discovery of a major ^{13}C spike in the Carnian (Late Triassic) linked to the eruption of Wrangellia flood basalts. *Geology*, 40: 79–82.
- Deczkowski, Z., 1997. Noryk i retyk. Sedimentacja, paleogeografia i paleotektonika. In: Marek, S. & Pajchlowa, M. (eds), *Epikontynetalny perm i moezozoik w Polsce. Prace Państwowego Instytutu Geologicznego*, 153: 187–194. [In Polish.]
- Dzik, J., Sulej, T. & Niedzwiedzki, G., 2008a. A dicynodont-theropod association in the latest Triassic of Poland. *Acta Palaeontologica Polonica*, 53: 733–738.
- Dzik, J., Niedzwiedzki, G. & Sulej, T., 2008b. Zaskakujące uwieńczenie ery gadów ssakosztalnych. *Ewolucja*, 3: 2–21. [In Polish.]
- Feist-Burkhardt, S., Götz, A. E., Szulc, J., Borkhataria, R., Geluk, M., Haas, J., Hornung, J., Jordan, P., Kempf, O., Michalik, J., Nawrocki, J., Reinhardt, L., Ricken, W., Röhling, H., G., Rüffer, T., Török, Á. & Zühlke, R., 2008. Triassic. In:

- McCann, T. (ed.), *The Geology of Central Europe. Vol. 2: Mesozoic and Cenozoic*. The Geological Society, London, pp. 749–822.
- Fijałkowska, A., 1994. Palynostratigraphy of the Lower and Middle Buntsandstein in NW part of the Holy Cross Mountains, Poland. *Geological Quarterly*, 38: 59–96.
- Fijałkowska-Mader, A., 2011. Palinostratigraphy of the Lower and Middle Buntsandstein in NW part of the Holy Cross Mountains, Poland. *Geological Quarterly*, 38: 59–96.
- Fijałkowska-Mader, A., 2011. Palinostratigraphy of the Lower and Middle Buntsandstein in NW part of the Holy Cross Mountains, Poland. In: Trela, W., Salwa, S. & Fijałkowska-Mader, A. (eds), Rekonstrukcje środowisk sedymencjinych na podstawie badań sedymentologicznych, geochemicznych i stratygraficznych. *Materiały VI Świętokrzyskich Spotkań Geologiczno-Geomorfologicznych, Ameliówka k. Kielc, 17–18 maja 2011 r.* Państwowy Instytut Geologiczny – Państwowy Instytut Badawczy, Oddział Świętokrzyski, Kielce, pp. 24–29. [In Polish.]
- Fijałkowska-Mader, A., Kuleta, M. & Zbroja, S., 2015. Lithostratigraphy, palynofacies and depositional environments of the Triassic deposits in the northern part of the Nida Basin, southern Poland. *Bulletyn Państwowego Instytutu Geologicznego* (in press). [In Polish, with English summary.]
- Fuglewicz, R. & Śnieżek, P., 1980. Upper Triassic megaspores from Lipie Śląskie near Lubliniec. *Przegląd Geologiczny*, 28: 459–461. [In Polish, with English title]
- Grauvogel-Stamm, L., 1969. Nouveaux types d'organes reproducteurs mâles de conifères du Grès à Voltzia (Trias inférieur) des Vosges. *Bulletin du Service de la Carte Géologique d'Alsace et de Lorraine*, 22: 93–120, 355–357.
- Grodzicka-Szymanko, W. & Orłowska-Zwolińska, T., 1972. Stratigraphy of the Upper Triassic in the NE margin of the Upper Silesian Coal Basin. *Kwartalnik Geologiczny*, 16: 216–232. [In Polish, with English summary.]
- Haas, J., Budai, T. & Raucsik, B., 2012. Climatic controls on sedimentary environments in the Triassic of the Transdanubian Range (Western Hungary). *Palaeogeography, Palaeoclimatology, Palaeoecology*, 353–355: 31–44.
- Hauschke, N. & Heunisch, C., 1989. Sedimentologische und palynologische Aspekte einer zyklisch entwickelten lakustrischen Sequenz im höheren Teil des Unteren Gipskeupers (km 1, Obere Trias) Nordwestdeutschlands. *Lippische Mitteilungen aus Geschichte und Landeskunde*, 58: 233–256.
- Hauschke, N. & Heunisch, C., 1990. Lithologie und Palynologie der Bohrung USB 3 (Horn – Bad Meinberg, Ostwestfalen): ein Beitrag zur Faziesentwicklung im Keuper. *Neues Jahrbuch für Geologie und Paläontologie – Abhandlungen*, 181: 79–105.
- Heunisch, C., 1990. Palynology of the well “Natzungen 1979”, map no 4321 Borgholz (Triassic: Upper Muschelkalk 2,3, Lower Keuper). *Neues Jahrbuch für Geologie und Paläontologie, Monatshefte 1990*: 17–42. [In German, with English abstract.]
- Heunisch, C., 1999. Die Bedeutung der Palynologie für Biostratigraphie und Fazies in der Germanischen Trias. In: Hauszke, N. & Wilde, V. (eds), *Trias. Eine ganz andere Welt. Mitteleuropa im frühen Erdmittelalter*. Dr. Friedrich Pfeil Press, Münschen, pp. 207–220.
- Heunisch, C. & Nitsch, E., 2011. Eine seltene Mikroflora aus der Mainhardt-Formation (Keuper, Trias) von Baden-Württemberg (Süddeutschland). *Jahresberichte und Mitteilungen des oberrheinischen geologischen Verrain, Neue Folge*, 93: 55–76.
- Heunisch, C., Luppold, F. W., Reinhardt, L. & Röhling, H. G., 2010. Palynofazies, bio- und Lithostratigrafie im grenzbereich Trias/Jura in der bohrung Mariental 1 (Lappwaldmulde, Ostniedersachsen). *Zeitschrift der Deutschen Gesellschaft für Geowissenschaften*, 161: 51–98.
- Kozur, H. W. & Bachmann, G. H., 2010. The Middle Carnian Wet Intermezzo of the Stuttgart Formation (Schilfsandstein), Germanic Basin. *Palaeogeography, Palaeoclimatology, Palaeoecology*, 290: 107–119.
- Kürschner, W. M. & Herngreen, G. F. W., 2010. Triassic palynology of central and northwestern Europe: a review of palynological diversity patterns and biostratigraphic subdivisions. In: Lucas, S. G. (ed.), *The Triassic Timescale. Geological Society of London Special Publication*, 334: 263–283.
- Lintnerová, O., Michalík, J., Uhlik, P., Soták, J. & Weisssová, Z., 2013. Latest Triassic climate humidification and kaolinite formation (Western Carpathians, Tatra Unit of the Tatra Mts.). *Geological Quarterly*, 57: 701–728.
- Mader, D., 1997. *Palaeoenvironmental Evolution and Bibliography of the Keuper (Upper Triassic) in Germany, Poland and Other Parts of Europe*. Loga, Köln, 1058 pp.
- Mader, D., 1990. *Palaeoecology of the Flora in Buntsandstein and Keuper in the Triassic of Middle Europe, 2. Keuper and Index*. Fischer, Stuttgart/New York, pp. 937–1582.
- Marcinkiewicz, T., 1981. On the question of megaspores from Lipie Śląskie. *Przegląd Geologiczny*, 39: 419–420. [In Polish.]
- Marcinkiewicz, T., Fijałkowska-Mader, A. & Pieńkowski, G., 2014. Megaspore zones of the epicontinental Triassic and Jurassic deposits in Poland – overview. *Bulletyn Państwowego Instytutu Geologicznego*, 457: 15–42. [In Polish, with English summary.]
- Michałik, J., Biroň, A., Lintnerová, O., Götz, A., E. & Ruckwied, K., 2010. Climate change at the Triassic/Jurassic boundary in the northwestern Tethyan realm, inferred from sections in the Tatra Mountains (Slovakia). *Acta Geologica Polonica*, 60: 535–548.
- Niedźwiedzki, G., Brusatte, S. L., Sulej, T. & Butler, R. J., 2014. Basal dinosauriform and theropod dinosaurs from the mid-late Norian (Late Triassic) of Poland: implications for Triassic dinosaur evolution and distribution. *Palaeontology*, 57: 1121–1142.
- Ogg, J., G., 2012. Triassic time scale. In: Gradstein, F., M., Ogg, J. G., Schmitz, M. D. & Ogg, G. M. (eds), *The Geologic Time Scale 2012. Vol. 2*. Elsevier, Amsterdam, pp. 700–730.
- Orłowska-Zwolińska, T., 1979. Miospores. In: Malinowska, L. (ed.), *Atlas skamieniałości przewodniczących i charakterystycznych. Budowa Geologiczna Polski, 3, cz. 2a: Mezozoik, Trias*. Wydawnictwa Geologiczne, Warszawa, pp. 166–200. [In Polish.]
- Orłowska-Zwolińska, T., 1981. Badania palinologiczne trias i ich znaczenie dla stratygrafia osadów w profilach obrzeżeń Górnego Świętokrzyskich i Górnosłaskiego Zagłębia Węglowego. In: *Fauna i flora triasu obrzeżenia Górnego Świętokrzyskich i Wyżyny Śląsko-Krakowskiej. Materiały V Krajowej Konferencji Paleontologów*, Kielce-Sosnowiec, pp. 61–66. [In Polish.]
- Orłowska-Zwolińska, T., 1983. Palynostratigraphy of the Upper part of Triassic epicontinental sediments in Poland. *Prace Instytutu Geologicznego*, 104: 1–89. [In Polish, with English summary.]
- Orłowska-Zwolińska, T., 1985. Palynological zones of the Polish epicontinental Triassic. *Bulletin Academy of Sciences, Earth Sciences*, 33: 107–119.
- Pieńkowski, G., Niedźwiedzki, G. & Brański, P., 2014. Climatic reversals related to the Central Atlantic magmatic province caused the end-Triassic biotic crisis — Evidence from continental strata in Poland. In: Keller, G. & Kerr, A. (eds), *Volcanism, Impacts, and Mass Extinctions: Causes and Effects*. Geological Society of America Special Papers, 505: 263–286.
- Pieńkowski, G. & Waksmundzka, M., 2009. Palynofacies In Lower Jurassic epicontinental deposits of Poland: tool to interpret sedimentary environments. *Episodes*, 32: 21–31.

- Powell, A. J., Dodge, J. D. & Lewis, J., 1990. Late Neogene to Pleistocene palynological facies of the Peruvian continental margin upwelling, Leg 112. In: Suess, E. & von Huene, R. (eds), *Proceedings of the Ocean Drilling Project, Scientific Results*, 112: 297–321.
- Preto, N., Kustatscher, E. & Wignall, P. B., 2010. Triassic climates – state of the art and perspectives. *Palaeogeography, Palaeoclimatology, Palaeoecology*, 290: 1–10.
- Roghi, G., Gianolla, P., Minarelli, L., Pilati, C. & Preto, N., 2010. Palynological correlation of Carnian humid pulses through western Tethys. *Palaeogeography, Palaeoclimatology, Palaeoecology*, 290: 89–106.
- Sadlok, G. & Wawrzyniak, Z., 2013. Upper Triassic vertebrate tracks from Kraków-Częstochowa Upland, Southern Poland. *Annales Societatis Geologorum Poloniae*, 83: 105–111.
- Środoń, J., Szulc, J., Anczkiewicz, A., Jewuła, K., Banaś, M. & Marynowski, L., 2014. Weathering, sedimentary, and diagenetic controls of mineral and geochemical characteristics of the vertebrate-bearing Silesian Keuper. *Clay Minerals*, 49: 569–594.
- Stanczko, K., 2007. Nowe dane paleobotaniczne na temat górnego triasu z Lipią Śląskiego koło Lublińca (południowa Polska). In: *Geo-Sympozjum Młodych Badaczy Silesia 2007*. Uniwersytet Śląski, Sosnowiec, pp. 157–170. [In Polish.]
- Świło, M., Niedźwiedzki, G. & Sulej, T., 2014. Mammal-like tooth from the Upper Triassic of Poland. *Acta Palaeontologica Polonica*, 59: 815–820.
- Szulc, J., Gradziński, M., Lewandowska, A. & Heunisch, C., 2006. The Upper Triassic crenogenic limestones in Upper Silesia (southern Poland) and their paleoenvironmental context. In: Alonso-Zarza, A. M. & Tanner, L. H. (eds), *Paleoenvironmental Record and Applications of Calcretes and Palustrine Carbonates*. Geological Society of America Special Paper, 416: 133–151.
- Szulc, J. & Racki, G., 2015. Grabowa Formation – the basic lithostratigraphic unit of the Upper Silesian Keuper. *Przegląd Geologiczny*, 63: 103–113. [In Polish, with English summary.]
- Szulc, J., Racki, G., Jewuła, K. & Środoń, J., 2015. How many Upper Triassic bone-bearing levels are there in Upper Silesia (southern Poland)? A critical review of stratigraphy and facies. *Annales Societatis Geologorum Poloniae*, 85: 587–626.
- Traverse, A., 2004. Proposal to conserve the fossil pollen morpho-generic name *Classopollis* against *Corollina* and *Circulina*. *Taxon*, 53: 847–848.
- Tyson, R. V., 1995. *Sedimentary Organic Matter. Organic Facies and Palynofacies*. Chapman and Hall, London, 615 pp.
- Vakhrameev, V. A., 1981. Pollen *Classopollis*: indicator of Jurassic and Cretaceous climates. *The Palaeobotanist*, 28–29: 301–307.
- Vakhrameev, V. A., 1987. Climates and distribution of some gymnosperms in Asia during the Jurassic and Cretaceous. *Review of Palaeobotany and Palynology*, 51: 205–212.
- Vakhrameev, V. A., 1991. *Jurassic and Cretaceous floras and climates of the Earth*. Cambridge University Press, Cambridge, 318 pp..
- Van Bergen, P. F. & Kerp, J. H. P., 1990. Palynofacies and sedimentary environments of a Triassic sections in southern Germany. In: Fermont, W. J. J. & Weegink, J. W. (eds), Proceedings International Symposium on Organic Petrology Zeist, The Netherlands, January 7–9, 1990. *Mededelingen Rijks Geologischen Dienst*, 45: 23–37.
- Ziegler, A. M., Parrish, J. M., Jiping, Y., Gyllenhaal, E. D., Rowley, D. B., Parrish, J. T., Shangyou, N., Bekker, A. & Hulver, M. L., 1994. Early Mesozoic phytogeography and climate. In: Allen, J. R. L., Hoskins, B. J., Sellwood, B. W., Spicer, R. A. & Valdes, P. J. (eds), *Palaeoclimates and Their Modeling*. Chapman and Hall, London, pp. 89–99.

Appendix 1 Annotated list of sporomorph taxa

(names of the index species are in bold print)

Miospores:

- aff. *Acanthotriletes* sp. (Fig. 8M)
Accinctisporites ligatus Leschik
Accinctisporites sp. (Fig. 9L)
 aff. *Accinctisporites* sp. (Fig. 14M)
Alisporites toralis (Leschik) Clarke (Figs 11H, 14U)
Alisporites sp. (Fig. 10C)
Anapiculatisporites spiniger (Leschik) Reinhart (Figs 12D, 14B)
Anapiculatisporites telephorus Pautsch (Figs 8L, 11B, 12C, 14C)
Anapiculatisporites sp.
Apiculatisporis firmus (Leschik) Orłowska-Zwolińska
Apiculatisporis sp.
Aratrisporites coryliseminis Klaus (Fig. 9E)
Aratrisporites fimbriatus (Klaus) Playford et Dettmann
Aratrisporites flexibilis Playford et Dettmann
Aratrisporites cf. *major* Mädler
Aratrisporites paraspinosus Klaus (Figs 7F, G, 9G, H)
Aratrisporites saturni (Thiergart) Mädler (Figs 7E, 9F)
Aratrisporites scabratus Klaus
***Aulisporites astigmosus* (Leschik) Klaus** (Figs 8F, G, 10I, J)
Aulisporites sp.
Baculatisporites sp. (Fig. 11U)
Brachysaccus neomundanus (Leschik) Mädler (Figs 7M, 13C)
Brachysaccus neomundanus (Leschik) Mädler var. minor
 Orłowska-Zwolińska
Brachysaccus sp.
Calamospora tener (Leschik) de Jersey (Fig. 8D)
Calamospora cf. *tener* (Leschik) de Jersey (Fig. 11N)
Calamospora sp. (Figs 11A, 14N)
 aff. *Callialasporites* sp. (Figs 7H, I, 9M)
 aff. *Camerosporites* sp. (Fig. 7C)
Carnisporites granulatus Schulz
Carnisporites mesozoicus (Klaus) Mädler
Carnisporites ornatus Mädler
Carnisporites sp. (Fig. 8H)
Caytonipollenites sp.
Cedripites microreticulatus Orłowska-Zwolińska
Cedripites sp.
***Classopollis meyeriana* (Klaus) de Jersey** (Fig. 13K, L)
Classopollis simplex (Danzé-Corsin et Laveine) Reiser et Williams
Classopollis torosus (Reissinger) Pflug
Conbaculatisporites mesozoicus Klaus (Figs 8N, 10K)
Conbaculatisporites sp. (Fig. 10L)
 aff. *Concentricipsorites* sp.
Conosmundasporites othmari Klaus (Fig. 8K)
 aff. *Conosmundasporites* sp. (Fig. 11S)
Con verrucosporites sp.
Corrugatisporites scanicus Nilsson (Figs 8O, 12F)
Corrugatisporites sp. (Fig. 10P)
Cyclotriletes sp. (Fig. 11T)
Deltoidospora minor (Couper) Pocock (Figs 8A, 12E)
Deltoidospora toralis (Leschik) Lund (Fig. 8B)
Deltoidospora sp. (Fig. 8C)
Densosporites cf. *fissus* (Reinhart) Schulz
Densosporites silesiensis Fijałkowska-Mader sp. nov. (Fig. 12M–O) (for description see Appendix 2)
Densosporites rogaliskai Fijałkowska-Mader sp. nov. (Fig. 12P) (for description see Appendix 2)

- Densosporites* sp., (Figs 7D, 9A, 12L, 14D, 14P)
Duplicisporites granulatus Leschik (Fig. 13J)
Enzonalarporites manifestus Leschik (Figs 9J, 11D)
Enzonalarporites vigens Leschik (Figs 9K, 13A)
Enzonalarporites sp.
Falcisporites sp. (Figs 13F, 14T)
Foveolatitriteles sp. (Fig. 12G)
aff. *Gibbeosporites* sp.
Geopolitis zwolinskae (Lund) Brenner
Granuloperculatipollis rufus Venkatachala et Goczán (Fig. 13M, N)
Illinites chitonoides Klaus
Illinites cf. *chitonoides* Klaus (Fig. 9N)
Inaperturopollenites sp.
Infernopolollenites sulcatus (Pautsch) Scheuring (Fig. 7L)
Kraeuselisporites cf. *cooksonae* (Klaus) Dettmann (Fig. 9B)
Kraeuselisporites lituus (Leschik) Scheuring (Fig. 9C)
Kraeuselisporites ramosus Leschik
Kraeuselisporites sp. (Figs 9D, 11C, 14R)
aff. *Kraeuselisporites* sp. (Fig. 13S)
Labiisporites triassicus Orłowska-Zwolińska (Figs 10G, 13G)
Leschikisporis aduncus (Leschik) Potonié
Lophotriteles sp.
Lunatisporites sp., (Fig. 14E, F, L)
Lycopodiadicidites kuepperi Klaus (Fig. 10M)
Lycopodiadicidites cf. *kuepperi* Klaus (Fig. 8R)
Lycopodiadicidites sp.
Lycopodiumsporites rugulatus (Couper) Schulz (Fig. 8P)
Marattisporites sp.
Micretriculatisporites opacus (Leschik) Klaus
Micretriculatisporites sp.
Monosaccites undetermined
Monsulcites minimus Cookson (Fig. 13O)
Monosulcites sp. (Fig. 13P)
aff. *Monosulcites* sp. (Fig. 14H)
Nevesisporites limatulus Playford (Figs 8U, 12I)
Neochomotriteles triangulatus (Bolchovitina) Reinhardt (Fig. 12J)
Neochomotriteles sp.
Neoraistrickia sp.
Nevesisporites bigranulatus (Levet-Carette) Morbey
Nevesisporites limatulus Playford (Figs 8U, 12I)
Nevesisporites lubricus Orłowska-Zwolińska
Ovalipollis longiformis Krutzsch
Ovalipollis lunensis Klaus (Fig. 9O)
Ovalipollis minimus Scheuring
Ovalipollis cf. *notabilis* Scheuring (Fig. 9P)
Ovalipollis ovalis Krutzsch (Figs 9R, 11F, G, 13B, T)
Ovalipollis rarus Klaus (Fig. 11E)
Ovalipollis sp. (Fig. 14G)
Palaeospongiosporis europaeus Schulz
Parillinites cf. *callosus* Scheuring
Parillintes vanus Scheuring (Fig. 7N)
Parillintes sp. (Figs 9U, 13D)
Partitisporites tenebrosus (Scheuring) Van der Eem
Partitisporites sp. (Fig. 13I)
aff. *Patinasporites* sp.
aff. *Perinopollenites* sp. (Fig. 7J)
aff. *Pinuspollenites* sp.
Platysaccus niger Mädler (Fig. 13E)
Platysaccus nitidus Pautsch (Fig. 10B)
Platysaccus papilionis Potonié et Klaus (Fig. 10A)
Platysaccus sp. (Fig. 11I)
Polycingulatisporites redundans (Bolchovitina) Playford et Dettmann (Fig. 12K)
Polycingulatisporites sp. (Fig. 10O)
aff. *Polypodiisporites* sp. (Fig. 12R)
Porcellispora longdonensis (Clarke) Scheuring (Figs 7A, B, 12B) *Porcellispora* sp. (Fig. 12B)
Praecirculina granifer (Leschik) Klaus
Protodiploxylinus sp. (Fig. 13H)
aff. *Protodiploxylinus* sp.
Protohaploxylinus sp. (Fig. 9S)
aff. *Protohaploxylinus* sp. (10G)
Pseudoenzonalasporites summus Scheuring
Reticulatisporites distinctus Orłowska-Zwolińska (Fig. 12H)
Reticulatisporites sp. (Figs 8S, 13R)
Retisulcites sp. (Fig. 9I)
Riccisporites tuberculatus Lundblad
aff. *Semiretisporis* sp. (Fig. 8T)
Sphagnumsporites sp.
Spiritisporites spirabilis Scheuring
Spore sp. A (Fig. 12U) (for description see Appendix 2)
Spore undetermined (10R, S)
Striatobabietites ayttugii Visscher (Fig. 9T)
Striatobabietites balmei Klaus (Fig. 7K)
Striatobabietites sp.
Taurocusporites cf. *morbeyi* Orłowska-Zwolińska (Fig. 12S)
Taurocusporites verrucatus Schulz (Figs 12T, 14O)
Taurocusporites sp.
aff. *Taurocusporites* sp. (Fig. 9A)
Todisporites cinctus (Maliavkina) Orłowska-Zwolińska (Figs 8E, 11R)
Todisporites sp.
aff. *Todisporites* sp. (Fig. 14A)
Triadispora crassa Klaus (Figs 7O, 11J)
Triadispora obscura Scheuring
Triadispora plicata Klaus (Fig. 7R)
Triadispora polonica Brugman (Figs 7S, 10D)
Tradispora suspecta Scheuring (Figs 7P, 10E, 11K)
***Triadispora verrucata* (Schulz) Scheuring** (Figs 7T, U)
Triadispora sp. (Figs 10F, 11L)
Uvaesporites argenteaformis (Bolchovitina) Schulz
Vallasportes ignacii (Leschik) Klaus
Vallasportes sp.
Verrucosisporites cf. *planus* Orłowska-Zwolińska
Verrucosisporites redactus Orłowska-Zwolińska (Figs 8J, 12A)
Verrucosisporites slevicensis (Mädler) Orłowska-Zwolińska
Verrucosisporites sp. (Figs 8I, 14S)
Zebrasporites sp. (Fig. 10N)
- Other palynomorphs:
Algae:
Botryococcus sp.
Schizosporis sp. (Figs 10H, 11M)
Dinoflagellata:
Dapcodinium cf. *priscum* Evitt
Fungal spores
- Reworked miospores:
aff. *Angustisulcites* sp.
Densoisporites nejburgii (Schulz) Balme (Fig. 11O)
Densoisporites cf. *nejburgii* (Schulz) Balme (Fig. 14J)
Densoisporites playfordii (Balme) Dettmann (Fig. 14I)
Densoisporites cf. *playfordii* (Schulz) Balme (Fig. 14J)
Densoisporites sp. (Fig. 10T)
Perotrilites minor Antonescu et Taugordeau-Lanz
aff. *Playfordiaspora* sp.
aff. *Punctatisporites* sp. (Fig. 14K)
Undetermined spore (Fig. 11P)
- Reworked planktonic forms:
Acritarcha undetermined (Fig. 13U)
? Chitinozoa (Fig. 10U)

Appendix 2**Descriptions of new taxa (Anna Fijalkowska-Mader)**

Descriptive terminology is after Punt *et al.* (1994).

Genus *Densosporites* Berry, 1937 emend. Butterworth, Jansonius, Smith et Staplin, 1964

Type species: *Densosporites covensis* Barry, 1937

Diagnosis: Trilete miospores triangular to subcircular in outline, two-layered, egzoexine on the proximal surface, evenly arched or with zona slightly raised above the central body.

Densosporites silesiensis sp. nov.

Fig. 12M, N, O

Derivation of name: Silesia – area, where the species was described for the first time.

Material: 10 specimens, Fig. 12N (holotype), housed in Polish Geological Institute – Polish Research Institute, Kielce Patoka1/137.9 (1).

Occurrence: Upper Silesia, Patoka 1 borehole, depth 137.9 m; Upper Triassic, Norian, Patoka Member of Grabowa Formation.

Description: Trilete spore with circular to subcircular outline. Outline of the central body convexly triangular to subcircular. Endoexine of central body thin, faintly roughened; laesure distinct with wide sutural ridges connected at their extremities to the zona. Ornamentation of egzoexine on the central proximal and distal areas consists of distinct regularly distributed verrucae. Verrucae are circular to irregular in shape. Sculpture of zone faintly granulose. Outline of the zone is smooth.

Dimensions: Equatorial diameter 30–40 µm (10 specimens).

Remarks: The proposed species differs from other *Densosporites* species in the presence of verrucae on the central proximal area. It differs from *D. verrucosus* Dybova et Jachowicz in its circular outline.

Densosporites rogalskai sp. nov.

Fig. 12P

Derivation of name: Maria Rogalska was a Polish palynologist, who for the first time described Lower Jurassic miospores from Upper Silesia.

Material: 4 specimens, Fig. 12P (holotype), housed in Polish Geological Institute – Polish Research Institute, Kielce Patoka1/134.6 (2).

Occurrence: Upper Silesia, Patoka 1 borehole, depth 134.6 m; Upper Triassic, Norian, Patoka Member of Grabowa Formation.

Description: Trilete spore with circular outline. Outline of the central body circular. Endoexine of central body thin faintly roughened; laesure distinct with wide sutural ridges connected at their extremities to the zona. Ornamentation of egzoexine on the central proximal and distal areas consists of distinct regularly distributed verrucae. Verrucae are circular to irregular in shape. Sculpture of zone verrucosed.

Dimensions: Equatorial diameter 30–40 µm (4 specimens).

Remarks: It differs from *Densosporites silesensis* in the rough outline of the zone and more irregular shape of the verrucae.

Spore sp. A

Fig. 12U

Spore circular in equatorial outline. Arms of trilete mark straight, bifurcated at the ends, extends to 5/6 of the proximal surface. Wide labrum continues into ridge surrounding the areas between arms of the trilete mark. Thickening of exine on the proximal side is arranged in regular pattern consisting of three trilobate elements. Spore outline is rough. Equatorial diameter 38 (1 specimen).

The single specimen the Patoka 1 borehole (depth 153.1 m) differs from other spores in the presence of regular, trilobate-shape ornamentation on the proximal areas between the labrum and exine ridge occurring on the equator and subcircular thickening of exine in the central part of trilete mark.